Empirical tsunami fragility modelling for hierarchical damage levels~~: An application to damage data of the 2009 South Pacific tsunami~~

Fatemeh Jalayer[1,2], Hossein ~~Ebrahimian[1]~~Ebrahimian[2], Konstantinos ~~Trevlopoulos[1]~~Trevlopoulos[2], Brendon ~~Bradley[2]~~Bradley[3]

[1]Institute for Risk and Disaster Reduction, University College London, Gower Street, London, WC1E 6BT, UK,
[2][1]Department of Structures for Engineering and Architecture, University of Naples Federico II, Naples 80125, Italy
[3][2]Department of Civil and Natural Resources Engineering, University of Canterbury, Private Bag 4800, Christchurch 8140, New Zealand

Correspondence to: Fatemeh Jalayer (fatemeh.jalayer@unina.it)

Abstract.

The present work proposes a simulation-based Bayesian method for parameter estimation and fragility model selection for mutually exclusive, and collectively exhaustive (MECE) damage states. This method uses adaptive Markov chain Monte Carlo simulation (MCMC) based on likelihood estimation using point-wise intensity values. It identifies the simplest model that fits the data best, among the set of viable fragility models considered. The proposed methodology is demonstrated for empirical fragility assessment for two different tsunami events and different classes of buildings with varying number of observed damage and flow depth data pairs. As ~~a~~ case-stud~~y~~ies, observed pairs of data for ~~tsunami intensity~~flow depth and corresponding damage level from the central South Pacific tsunami on September 29, 2009~~-~~, and Sulawesi-Palu Tsunami on 28 September, 2018 ~~,~~are used. ~~The tsunami was triggered by an unprecedented earthquake doublet (Mw 8.1 and Mw 8.0) and seriously impacted numerous locations in the central South Pacific.~~ Damage data related to~~-~~ a total of 5 different building classes ~~a~~were analyzed~~120 brick masonry residential buildings in American Samoa and Samoa islands were utilized~~. It is shown that the proposed methodology is stable and efficient for data sets with a very low number of damage versus intensity data pairs and cases in which observed data are missing for some of the damage levels.~~ A six-tier damage scale was considered, using tsunami flow depth as the intensity measure.~~

Keywords: probabilistic tsunami risk assessment, tsunami fragility, Bayesian inference, model class selection

1 Introduction

Fragility models express the probability of exceeding certain damage thresholds for a given level of intensity for a specific class of buildings or infrastructure. Empirical fragility curves are models derived based on observed pairs of damage and intensity data for buildings and infrastructures usually collected, acquired, and even partially simulated in the aftermath of disastrous events. Some examples of empirical fragility models are: seismic fragility (Rota et al. 2009, Rosti et al. 2021), tsunami fragility (Koshimura et al. 2009a, Reese et al. 2011; a comprehensive review can be found in Charvet et al. 2017), flooding fragility (Wing et al. 2020), and debris flow fragility curves (Eidsvig et al. 2014). Empirical fragility modelling is greatly affected by how the damage and intensity parameters are defined. Mutually exclusive and collectively exhaustive (MECE, see next section for the definition) damage states are quite common in the literature as discrete physical damage states. The MECE condition is necessary

for damage states in most probabilistic risk formulations leading to the mean rate of exceeding loss (e.g., Behrens et al. 2021).

45   Tsunami fragility curves usually employ the tsunami flow depth as the measure of intensity; although different studies use also other measures like current velocity (e.g., De Risi et al. 2017b, Charvet et al. 2015). Charvet et al. (2015) demonstrate that the flow depth may cease to be an appropriate measure of intensity for higher damage states and other parameters such as the current velocity, debris impact, and scour can become increasingly more important. De Risi et al. (2017b) developed bivariate tsunami

50   fragilities, which account for the interaction between the two intensity measures, tsunami flow depth and current velocity.

Early procedures for empirical tsunami fragility curves used data binning for representing the intensity. For example, Koshimura et al. (2009b) binned the observations by the intensity measure, i.e., the flow depth, however the latest procedures have mostly used point-wise intensity estimates instead.

55   Fragility curves for MECE damage states are distinguished by their nicely "laminar" shape; in other words, the curves should not intersect. When fitting empirical fragility curves to observed damage data, this condition is not satisfied automatically. For example, fragility curves are usually fitted for individual damage states separately and they are filtered afterwards to remove the crossing fragility curves (e.g., Miano et al. 2020) or ordered ("parallel") fragility models are used from the start (Charvet

60   et al. 2014, Lahcene et al. 2021). Charvet et al. (2014) and De Risi (2017a) also used partially ordered models to derive fragility curves for MECE damage states. They used the multinomial probability distribution to model the probability of being in any of MECE damage states based on binned intensity representation. De Risi et al. (2017a) used Bayesian inference to derive the model parameters for an ensemble of fragility curves.

65   Empirical tsunami fragility curves are usually constructed using generalized linear models based on probit, logit, or the complementary loglog link functions (Charvet et al. 2014, Lahcene et al. 2021). As far as the assessment of the goodness of fit, model comparison and selection are concerned, approaches based on the likelihood ratio and Akaike Information Criterion, (e.g., Charvet et al. 2014, Lahcene et al. 2021) and on k-fold cross validation have also been used (Chua et al. 2021). For estimating

70   confidence intervals for empirical tsunami fragility curves, bootstrap resampling has been commonly used (Charvet et al. 2014, Lahcene et al. 2021, Chua et al. 2021).

The present paper presents a simulation-based Bayesian method for inference and model class selection for the ensemble modelling of the tsunami fragility curves for MECE damage states for a given class of buildings. By fitting the (positive definite) fragility link function to the conditional probability of

75   being in a certain damage state, given that building is not in any of the preceding states, the method ensures that the fragility curves do not cross (i.e., they are "hierarchical" as in De Risi et al. 2017a). The method uses adaptive Markov Chain Monte Carlo Simulation (MCMC, Beck and Au 2002), based on likelihood estimation using point-wise intensity values, to infer the ensemble of the fragility model parameters. Alternative link functions are compared based on log evidence which considers both the

80   average goodness of fit (based on log likelihood) and the model parsimony (based on relative entropy). This way, among the set of viable models considered, it identifies the simplest model that fits the data best. By "simplest model", we mean the model having maximum relative entropy (measured using the Kullback-Leibler (Kullback and Leibler 1951) distance) with respect to the data. This usually means the model has a small number of parameters.

85

The main advantage is that the method provides, within the same set of runs, consistent parameter estimations for all the damage states, estimates confidence intervals, and identifies the best fragility model class among the pool of models. Although the application is demonstrated for the observed

4~~2~~ Methodology

4.1~~2.1~~ Definitions of intensity and damage parameters

The intensity measure, IM, (or simply "intensity"; e.g., the tsunami flow depth) refers to a parameter used to convey information about an event from the hazard level to the fragility level –it is an intermediate variable. The damage parameter, D, is a discrete random variable and the vector of damage levels is expressed as $\{D_j, j=0:N_{DS}\}$, where D_j as the jth *damage level (threshold)* and N_{DS} as the total number of damage levels considered (depending on the damage scale being used and on the type of hazard, e.g., earthquake, tsunami, debris flow). Normally, D_0 denotes the *no-damage* threshold, while $D_{N_{DS}}$ defines the total *collapse* or *being totally washed away*. Let us assume that DS_j is the jth *damage state* defined by the logical statement that the damage D is between the two damage thresholds D_j and D_{j+1}; i.e., D is equal to or greater than D_j and smaller than D_{j+1} as follows (see also Figure 1 for a graphical representation of the above expressions):

$$DS_j \equiv \left(D \geq D_j\right) \cdot \left(D < D_{j+1}\right) \tag{1}$$

where $(\cdot)$ denotes the logical product and is read as "AND". Obviously, for the last damage state, we have $DS_{N_{DS}} \equiv D \geq D_{N_{DS}}$.
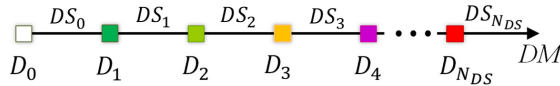
Figure 1: Graphical representation of damage levels D_j and damage states DS_j, where $j=0:N_{DS}$

Damage states $\{DS_0, DS_1, \dots, DS_{N_{DS}}\}$ are mutually exclusive and collectively exhaustive (MECE) if an only if $P\left(DS_i \cdot DS_j \middle| IM\right) = 0$ (if $i \neq j$, $j = 0: N_{DS}$) and $\sum_{j=0}^{N_{DS}} P\left(DS_j \middle| IM\right) = 1$; $(\cdot)$ denotes the logical product and is read as "AND". In simple words, the damage states are MECE if being in one damage state excludes all others and if all the damage states together cover the entire range of possibilities in terms of damage. The ensemble of MECE damage states DS_j, $j=0:N_{DS}$ is usually referred to as the *damage scale* (e.g., the EMS98, Grünthal 1998)

The proposed methodology herein is also applicable to fragility assessment in cases where observed damage data is not available for some of damage levels. Let **index** be the vector of j values ($j=0: N_{DS}$) indicating damage levels N_i for which observed data is available (j values are in ascending order). The new damage scale formed as $\{DS_{\textbf{index}(1)}, DS_{\textbf{index}(2)}, \dots, DS_{\textbf{index}(N)}\}$, where N is the length of vector **index**, ~~i~~is also MECE. It is noteworthy that the number of fragility curves derived in this case is going to be equal to $N-1$. In the following, for simplicity and without loss of generality, we have assumed that observed data is available for all damage levels, i.e., **index**$=\{0~~0~~:N_{DS}\}$, that is, $N_{DS}=N_{DS}-1$. However, the proposed methodology is also applicable to the modified damage scale formed by damage level indices in vector **index**$(1:N~~+1~~)$. We will later see examples of such application in the case studies.

4.22.2 Fragility modelling using generalized regression models

The generalized regression models (GLM) are more suitable for empirical fragility assessment with respect to the standard regression models. This is mainly because the dependent variable in the case of the generalized regression models is a Bernoulli binary variable (i.e., only two possible values: 0 or 1). Bernoulli variables are particularly useful in order to detect whether a specific damage level is exceeded or not (only two possibilities). In the following, fragility assessment based on GLM's is briefly described.

The term $P(DS_j|IM)$ denotes the probability of being in damage state DS_j for a given intensity level IM. Based on N_{DS} damage thresholds, tThis conditional probability $P(DS_j|IM)$ can be read (see Equation 1) as the probability that $(D \geq D_j)$ and $(D < D_{j+1})$, and can be estimated as follows (see Appendix A for the derivation):

$$P(DS_j|IM) = P\left[(D \geq D_j) \cdot (D < D_{j+1})|IM\right]$$
$$= \begin{cases} P(D \geq D_j|IM) - P(D \geq D_{j+1}|IM) & \text{for } 0 \leq j < N_{DS} \\ P(D \geq D_j|IM) & \text{for } j = N_{DS} \end{cases} \tag{2}$$

where $P(D \geq D_j|IM)$ is the *fragility function* for damage level D_j.

For each damage threshold, fragility can be obtained for a desired building class considering that the damage data provides Bernoulli variables (binary values) of whether the considered damage level was exceeded or not for given IM levels. For damage threshold D_j, all buildings with an observed damage level $D < D_j$ will have a probability equal to zero, while those with $D \geq D_j$ will have an assigned probability equal to one. In other words, for building i and damage state j, the Bernoulli variable Y_{ij} indicates whether building i is in damage state j:

$$Y_{ij} = \begin{cases} 1 & \text{if building } i \text{ exceeds } D_j & \text{with probability } P(D \geq D_j|IM_i) \\ 0 & \text{if building } i \text{ does not exceed } D_j & \text{with probability } 1 - P(D < D_j|IM_i) \end{cases} \tag{3}$$

where IM_i is the intensity evaluated at the location of building i. A Bernoulli variable is defined by one parameter which is $P(D \geq D_j|IM_i)$ herein. This latter is usually linked to a linear logarithmic predictor in the form:

$$l_{ij} = \alpha_{0,j} + \alpha_{1,j} \ln IM_i \tag{4}$$

$$l_{ij} = \alpha_{0,j} + \alpha_{1,j} \ln IM_i \tag{4}$$

where $\alpha_{0,j}$ and $\alpha_{1,j}$ are regression constants for damage level j. We have employed generalized linear regression (e.g., Agresti 2012) with different link functions "logit", "probit", and "cloglog", to define probability function π_{ij} as following:

cloglog (complementary log-log) transformation, the link function at the location of building *i* can be
160 expressed as $l_{ij} = \ln[-\ln(1 - \pi_{ij})]$. It is noted that the generalized linear regression based on maximum likelihood estimation (MLE) is available in many statistical software packages (e.g., MathWorks, Python, R).

-In the following, we have referred to the general methodology of fitting fragility model to data –one damage state at a time— the "*Basic method*". In the Basic method, the probability of exceeding damage
165 level *j* is equal to the probability function defined in Equation (5); that is, $\pi_{ij} = P(D \geq D_j|IM_i)$. This method for empirical fragility curve parameter estimation is addressed in detail in the Section "*Results*", under "MLE-*Basic*" method. The fragility curves obtained under the "MLE-*Basic*" method could potentially cross, leading to the ill condition that $P(DS_j|IM) < 0$. To overcome this, a *hierarchical fragility modeling approach* has been adopted like that in De Risi et al. (2017a).

170 **4.32.3 Hierarchical fragility modelling**

Equation (2) for $0 \leq j < N_{DS}$, and given IM_i, can also be written as follows using the product rule in probability:

$$P(DS_j|IM_i) = P[(D < D_{j+1}) \cdot (D \geq D_j)|IM_i]$$
$$= [1 - P(D \geq D_{j+1}|D \geq D_j, IM_i)] \cdot P(D \geq D_j|IM_i) \tag{6}$$

The term $P(D \geq D_{j+1}|D \geq D_j, IM_i)$ embedded in Equation (6) denotes the conditional probability that
175 the damage exceeds the damage threshold D_{j+1} knowing that it has already exceeded the previous damage level D_j given IM_i. By making $\pi_{ij} = P(D \geq D_{j+1}|D \geq D_j, IM_i)$ (see Equation 5, which is positive definite), we ensure that the fragility curve of a lower damage level will not fall below the fragility curve of the subsequent damage threshold (the ill condition of $P(DS_j|IM) < 0$ does not take place). Hence, Equation (6) can be expanded as follows (see Appendix B for derivation):

180
$$P(DS_j|IM_i) = (1 - \pi_{ij}) \cdot \left[1 - \sum_{k=0}^{j-1} P(DS_k|IM_i)\right] \quad \text{for } j \geq 1 \tag{7}$$
$$P(DS_0|IM_i) = 1 - \pi_{i0} = P(D < D_1)$$

$$P(DS_j|IM_i) = \begin{cases} (1 - \pi_{ij}) \cdot \left[1 - \sum_{k=0}^{j-1} P(DS_k|IM_i)\right] & \text{for } j \geq 1 \\ 1 - \pi_{i0} \triangleq P(D < D_1|IM_i) & \text{for } j = 0 \end{cases} \tag{7}$$

In this way, the fragility curves are constructed in a hierarchical manner by first constructing the "fragility increments" $P(DS_j|IM_i)$. ~~starting from *j=0*.~~ Note that for the last damage state $DS_{N_{DS}}$, the probability $P(DS_{N_{DS}}|IM_i\text{IM})$, which is also equal to the fragility of the ultimate damage threshold
185 $D_{N_{DS}}$, i.e. $P(D \geq D_{N_{DS}}|IM)$ (see Equation 2), can be estimated by satisfying the CE condition:

$$P(DS_{N_{DS}}|IM_i) = P(D \geq D_{N_{DS}}|IM_i) = 1 - \sum_{j=0}^{N_{DS}-1} P(DS_j|IM_i) \tag{8}$$

Accordingly, the fragility for other damage levels $P(D \geq D_j|IM_i)$, where $0 < j < N_{DS}$, can be obtained from Equation (2) by starting from the fragility of the higher threshold $P(D \geq D_{j+1}|IM)$, and adding successively $P(DS_j|IM)$ (see Equation 7) as follows:

$$190 \quad P\left(D \ge D_j \middle| IM_i\right) = P\left(DS_j \middle| IM_i\right) + P\left(D \ge D_{j+1} \middle| IM_i\right) \quad \text{for } 0 \le j < N_{DS} \tag{9}$$

As a result, the set of hierarchical fragility models based on Equation (9) has $2 \times N_{DS}$ model parameters with the vector $\boldsymbol{\theta} = \left[\{\alpha_{0,j}, \alpha_{1,j}\}, j = 0: N_{DS} - 1\right]$. Obviously, with reference to Equation (8), no model parameter is required for the last damage level which is derived by satisfying the CE condition. The vector $\boldsymbol{\theta}$ of the proposed hierarchical fragility models can be defined by two different approaches:

195 1) *MLE method*: a generalized linear regression model (as explained in previous section) is used for the conditional fragility term $\pi_{ij} = P\left(D \ge D_{j+1} \middle| D \ge D_j, IM\right)$ for the jth damage state DS_j (see Equation 7, $0 \le j < N_{DS}$). Herein, we need to work with partial damage data so that all buildings in DS_j (with an observed damage $D_j \le D < D_{j+1}$) will be assigned a probability equal to zero, while those in higher damage states (with $D \ge D_{j+1}$) will be assigned a probability equal to one
200 (i.e., in order to model the conditioning on $D \ge D_j$, the domain of possible damage levels is reduced to $D \ge D_j$).
2) *Bayesian model class selection* (*BMCS*): employing the Bayesian inference for model updating to obtain the joint distribution of the model parameters.

Detailed discussion about these two approaches, namely "MLE" and "BMCS", for parameters
205 estimation of empirical fragility curves are provided in Section "*Results*".

4.42.4 Bayesian model class selection (BMCS) and parameter inference using adaptive MCMC

We use the Bayesian model class selection (BMCS) herein to identify the best link model to use in the generalized linear regression scheme. However, the procedure is general and can be applied to a more
210 diverse pool of candidate fragility models. BMCS (or model comparison) is essentially Bayesian updating at the model class level to make comparisons among candidate model classes given the observed data (e.g., Beck and Yuen 2004, Muto and Beck 2008). Given a set of $N_{\mathbb{M}}$ candidate model classes $\{\mathbb{M}_k, k = 1: N_{\mathbb{M}}\}$, and in the presence of the data $\mathbf{D}$, the posterior probability of the kth model class, denoted as $P(\mathbb{M}_k|\mathbf{D})$ can be written as follows:

$$215 \quad P\left(\mathbb{M}_k \middle| \mathbf{D}\right) = \frac{p\left(\mathbf{D}\middle|\mathbb{M}_k\right)P\left(\mathbb{M}_k\right)}{\sum_{k=1}^{N_{\mathbb{M}}} p\left(\mathbf{D}\middle|\mathbb{M}_k\right)P\left(\mathbb{M}_k\right)} \tag{10}$$

In lieu of any initial preferences about the prior $P(\mathbb{M}_k)$, one can assign equal weights to each model; thus, $P(\mathbb{M}_k) = 1/N_{\mathbb{M}}$. Hence, the probability of a model class is dominated by the likelihood $p(\mathbf{D}|\mathbb{M}_k)$ (a.k.a. *evidence*). It is to note that p herein stands for the probability density function (PDF). Here data vector $\mathbf{D} = \{(IM, DS)_i, i = 1: N_{CL}\}$ defines the observed intensity and damage data for N_{CL} buildings
220 surveyed for class *CL*. ~~In this paper, we are considering a mono-class portfolio of buildings.~~ Let us define the vector of model parameters $\boldsymbol{\theta}_k$ for model class $\mathbb{M}_k$ as $\boldsymbol{\theta}_k = \left[\{\alpha_{0,j}, \alpha_{1,j}\}_k, j = 0: N_{DS} - 1\right]$. We use the Bayes theorem to write the "*evidence*" $p(\mathbf{D}|\mathbb{M}_k)$ provided by data $\mathbf{D}$ for model $\mathbb{M}_k$ as follows:

$$p\left(\mathbf{D}\middle|\mathbb{M}_k\right) = \frac{p\left(\mathbf{D}\middle|\boldsymbol{\theta}_k, \mathbb{M}_k\right) p\left(\boldsymbol{\theta}_k\middle|\mathbb{M}_k\right)}{p\left(\boldsymbol{\theta}_k\middle|\mathbf{D}, \mathbb{M}_k\right)} \tag{11}$$

225 It can be shown (see Appendix C, Muto and Beck 2008) that logarithm of the evidence (called *log-evidence*) $\ln[p(\mathbf{D}|\mathbb{M}_k)]$ can be written as:

$$\ln\Big[\,p\big(\mathbf{D}|\mathbb{M}_k\big)\Big] = \underbrace{\int_{\Omega_{\theta_k}} \ln\Big[\,p\big(\mathbf{D}|\theta_k,\mathbb{M}_k\big)\Big]p\big(\theta_k|\mathbf{D},\mathbb{M}_k\big)\mathrm{d}\theta_k}_{\text{Term 1}} - \underbrace{\int_{\Omega_{\theta_k}} \ln\Bigg[\frac{p\big(\theta_k|\mathbf{D},\mathbb{M}_k\big)}{p\big(\theta_k|\mathbb{M}_k\big)}\Bigg]p\big(\theta_k|\mathbf{D},\mathbb{M}_k\big)\mathrm{d}\theta_k}_{\text{Term 2}} \quad (12)$$

where Ω_{θ_k} is the domain of θ_k, and $p(\mathbf{D}|\theta_k,\mathbb{M}_k)$ is the likelihood function conditioned on model class $\mathbb{M}_k$. "*Term* 1" denotes the posterior mean of the log-likelihood, which is a measure of the average data
230 fit to model $\mathbb{M}_k$. "*Term* 2" is the relative entropy (Kullback and Leibler 1959, Cover and Thomas 1991) between the prior $p(\theta_k|\mathbb{M}_k)$ and the posterior $p(\theta_k|\mathbf{D},\mathbb{M}_k)$ of θ_k given model $\mathbb{M}_k$, which is a measure of the distance between the two PDFs. The latter *Term* 2 measures quantitatively the amount of information (on average) that is "gained" about θ_k from the observed data $\mathbf{D}$. It is interesting that *Term* 2 in the log-evidence expression penalizes for model complexity; i.e., if the model extracts more
235 information from data (which is a sign of being a complex model with more model parameters), the log-evidence reduces. The exponential of the log-evidence, $p(\mathbf{D}|\mathbb{M}_k)$, is going to be implemented directly in Equation (10), to provide the probability attributed to the model class $\mathbb{M}_k$. More details on how to estimate the two terms in Equation (12) are provided in the Section "*Results*".
The likelihood $p(\mathbf{D}|\theta_k,\mathbb{M}_k)$ can be derived, based on point-wise intensity information, as the likelihood
240 of $n_{CL,j}$ buildings being in damage state DS_j (considering that $\sum_{j=0}^{N_{DS}} n_{CL,j} = N_{CL}$), according to data $\mathbf{D}$ defined before:

$$p(\mathbf{D}|\theta_k,\mathbb{M}_k) = \prod_{j=0}^{N_{DS}}\prod_{i=1}^{n_{CL,j}} P\big(DS_j|IM_i\big) \quad (13)$$

The posterior distribution $p(\theta_k|\mathbf{D},\mathbb{M}_k)$ can be found based on Bayesian inference:

$$\underbrace{p\big(\theta_k|\mathbf{D},\mathbb{M}_k\big)}_{\text{posterior}} = \frac{p\big(\mathbf{D}|\theta_k,\mathbb{M}_k\big)p\big(\theta_k|\mathbb{M}_k\big)}{\int_{\Omega_{\theta_k}} p\big(\mathbf{D}|\theta_k,\mathbb{M}_k\big)p\big(\theta_k|\mathbb{M}_k\big)\mathrm{d}\theta_k} = C^{-1}\underbrace{p\big(\mathbf{D}|\theta_k,\mathbb{M}_k\big)}_{\text{likelihood}}\underbrace{p\big(\theta_k|\mathbb{M}_k\big)}_{\text{prior}} \quad (14)$$

245 where C^{-1} is a normalizing constant. In lieu of additional information (or preferences), the prior distribution, $p(\theta_k|\mathbb{M}_k)$, can be estimated as the product of marginal normal/lognormal PDFs for each model parameter, i.e., a multivariate normal/lognormal distribution with zero correlation between the pairs of model parameters θ_k (see Appendix D). More detail about an efficient prior joint PDF is provided in the Section "*Results*". To sample from the posterior distribution $p(\theta_k|\mathbf{D},\mathbb{M}_k)$ in Equation
250 (1514), an *adaptive* MCMC simulation routine (see Appendix E) is employed. MCMC is particularly useful for drawing samples from the target posterior, while it is known up to a scaling constant C^{-1} (see Beck and Au 2002); thus, in Equation (14), we only need un-normalized PDFs to feed the MCMC procedure. The MCMC routine herein employs the Metropolis-Hastings (MH) algorithm (Metropolis et al. 1953, Hasting 1970) to generate samples from the target joint posterior PDF $p(\theta_k|\mathbf{D},\mathbb{M}_k)$.

255 ### 4.52.5 Calculating the hierarchical fragilities and the corresponding confidence intervals based on the vector of model parameters θ_k

For each realization of the vector of model parameters θ_k, the corresponding set of hierarchical fragility curves can be derived based on the procedure described in the previous sections. Since we have N_d realizations of the model parameters drawn from the joint PDF $p(\theta_k|\mathbf{D},\mathbb{M}_k)$ (where N_d isbased on the
260 number of distinct samples drawn from adaptive MCMC procedure, see also Appendix E), we can use the concept of *Robust Fragility* (RF) proposed in Jalayer et al. 2017 (see also Jalayer et al. 2015, and

Jalayer and Erahimian 2020) to derive confidence intervals for the fragility curves. RF is defined as the expected value for a prescribed fragility model considering the joint probability distribution for the fragility model parameters $\boldsymbol{\theta}_k$. The RF herein can be expressed as:

265
$$P\left(D \geq D_j \middle| IM, \mathbf{D}, \mathbb{M}_k\right) = \int_{\Omega_{\boldsymbol{\theta}_k}} P\left(D \geq D_j \middle| IM, \boldsymbol{\theta}_k\right) p\left(\boldsymbol{\theta}_k \middle| \mathbf{D}, \mathbb{M}_k\right) \mathrm{d}\boldsymbol{\theta}_k = \mathbb{E}_{\boldsymbol{\theta}_k|\mathbf{D},\mathbb{M}_k}\left[P\left(D \geq D_j \middle| IM, \boldsymbol{\theta}_k\right)\right] \quad (15)$$

$$P\left(D \geq D_j \middle| IM, \mathbf{D}, \mathbb{M}_k\right) = \int_{\Omega_{\boldsymbol{\theta}_k}} P\left(D \geq D_j \middle| IM, \boldsymbol{\theta}_k\right) p\left(\boldsymbol{\theta}_k \middle| \mathbf{D}, \mathbb{M}_k\right) \mathrm{d}\boldsymbol{\theta} = \mathbb{E}_{\boldsymbol{\theta}_k|\mathbf{D},\mathbb{M}_k}\left[P\left(D \geq D_j \middle| IM, \boldsymbol{\theta}_k\right)\right] \quad (15)$$

where $P\left(D \geq D_j \middle| IM, \boldsymbol{\theta}_k\right)$ is the fragility given the model parameters $\boldsymbol{\theta}_k$ associated with the model $\mathbb{M}_k$ (it has been assumed that once conditioned on fragility model parameters $\boldsymbol{\theta}_k\boldsymbol{\theta}$, the fragility becomes

270 independent of data $\mathbf{D}$); $\mathbb{E}_{\boldsymbol{\theta}_k|\mathbf{D},\mathbb{M}_k}$ is the expected value over the vector of fragility parameters $\boldsymbol{\theta}_k$ for model $\mathbb{M}_k$. The integral in Equation (15) can be solved numerically by employing Monte Carlo simulation with N_d ~~simulations~~ generated samples ~~of~~from the vector $\boldsymbol{\theta}_k$ as follows:

$$P\left(D \geq D_j \middle| IM, \mathbf{D}, \mathbb{M}_k\right) \cong \frac{1}{N_d} \sum_{l=1}^{N_d} P\left(D \geq D_j \middle| IM, \boldsymbol{\theta}_{k,l}\right) \quad (16)$$

275 where $P\left(D \geq D_j \middle| IM, \boldsymbol{\theta}_{k,l}\right)$ is the fragility given the lth realization $(l = 1:N_d)$ of the model parameters $\boldsymbol{\theta}_k$ for model $\mathbb{M}_k$. Based on the definition represented in Equation (15) and Equation (16), the variance $\sigma^2_{\boldsymbol{\theta}_k|\mathbf{D},\mathbb{M}_k}$, which can be used to estimate a confidence interval for the fragility considering the uncertainty in the estimation of $\boldsymbol{\theta}_k$, is calculated as follows:

$$\sigma^2_{\boldsymbol{\theta}_k|\mathbf{D},\mathbb{M}_k}\left[P\left(D \geq D_j \middle| IM, \boldsymbol{\theta}_k\right)\right] = \underbrace{\mathbb{E}_{\boldsymbol{\theta}_k|\mathbf{D},\mathbb{M}_k}\left[P\left(D \geq D_j \middle| IM, \boldsymbol{\theta}_k\right)^2\right]}_{\cong \frac{1}{N_d}\sum_{i=1}^{N_d} P\left(D \geq D_j|IM, \boldsymbol{\theta}_{k,l}\right)^2} - \underbrace{\left(\mathbb{E}_{\boldsymbol{\theta}_k|\mathbf{D},\mathbb{M}_k}\left[P\left(D \geq D_j \middle| IM, \boldsymbol{\theta}_k\right)\right]\right)^2}_{= P\left(D \geq D_j|IM, \mathbf{D}, \mathbb{M}_k\right)^2 \text{ (Eq.16)}} \quad (17)$$

280 The empirical fragilities derived through the hierarchical fragility procedure are not necessarily attributed to a lognormal distribution. Hence, we have derived equivalent lognormal statistics (i.e., the median and dispersion) for the resulting fragility curves. The median intensity, η_{IM_C}, for a given damage level, is calculated as the IM corresponding to 50% probability on the fragility curve. The logarithmic standard deviation (dispersion) of the equivalent lognormal fragility curve at the onset of damage

285 threshold, β_{IM_C}, is estimated as half of the logarithmic distance between the IMs corresponding to the probabilities of 16% (IM_C^{16}) and the 84% (IM_C^{84}) on the fragility curve; thus, the dispersion can be estimated as $\beta_{IM_C} = 0.50 \times \ln\left(IM_C^{84}/IM_C^{16}\right)$. The overall effect of epistemic uncertainties (due to the uncertainty in the fragility model parameters and reflecting the effect of limited sample size) on the median of the empirical fragility curve is considered through (logarithmic) intensity-based standard

290 deviation denoted as β_{UF} (see Jalayer et al. 2020). β_{UF} can be estimated as half of the (natural) logarithmic distance (along the IM axis) between the median intensities (i.e., 50% probability) of the RF'~~curves~~s derived with ~~a~~ 16% ~~confidence level~~ (denoted as IM^{84}) and 84% ~~confidence level~~ (IM^{16}) confidence levels, respectively; i.e., $\beta_{UF} = 0.50 \times \ln\left(IM^{84}/IM^{16}\right)$. The RF and its confidence band, the sample fragilities $\boldsymbol{\theta}_{k,l}$ (where $l = 1:N_d$), the equivalent lognormal parameters ~~of the RF~~ η_{IM_C} and

295 β_{IM_C}, of the RF, the epistemic uncertainty β_{UF}, and finally the intensities IM^{16} and IM^{84} are shown in Figure 2d to Figure 64d in the following Section 3.

~~5~~ 3 Results

~~5.1~~ 3.1 Case Stud~~y 1~~y: The 2009 South Pacific Tsunami

The central South Pacific region-wide tsunami was triggered by an unprecedented earthquake doublet (Mw 8.1 and Mw 8.0) on September 29, 2009, between about 17:48 and 17:50 UTC (Goff and Dominey-Howes 2009). The tsunami seriously impacted numerous locations in the central South Pacific. Herein, the damage data related to the brick masonry ~~masonry~~ residential ~~buildings~~ (1 storey) and Timber residential buildings associated with the reconnaissance survey sites of American Samoa and Samoa islands were utilized ~~as a proof of concept. Out of N_{CL}=120 surveyed buildings in the class of masonry residential, 84 were in American Samoa, and 36 in Samoa.~~ Based on the observed damage regarding different indicators (see Reese et al. 2011 for more details on damage observation), each structure was assigned a damage state between (DS_0 and DS_5). The original data documented in Reese et al. (2011) reporting the tsunami flow depth and the attributed damage state to each surveyed building can be found on the site of the European Tsunami Risk Service (https://eurotsunamirisk.org/datasets/~~, reported as Class 1: brick masonry residential~~). The five damage states~~levelsthresholds~~ (N_{DS} = 5 ~~not counting DS_0~~) and a description of the indicators leading to the classification of the damage states are given in Table 1 based on Reese et al. (2011).

Table 1. The classification of damage thresholds (the damage scale) used ~~in this study and the observed damage data associated with residential masonry buildings~~ for 2009 South Pacific ~~Data~~Tsunami (from Reese et al. 2011).

Damage Level		Damage level description
D_0	None	no damage
D_1	Light	non-structural damage
D_2	Minor	significant non-structural damage, minor structural damage
D_3	Moderate	significant structural and non-structural damage
D_4	Severe	irreparable structural damage, will require demolition
D_5	Collapse	complete structural collapse

Damage threshold		Damage level description	Number of masonry buildings $n_{CL,j}$	Flow depth range (m)*
D_0	None	no damage	9	[0.01-0.50]
D_1	Light	non-structural damage	3	[0.30-0.80]
D_2	Minor	significant non-structural damage, minor structural damage	23	[0.40-2.00]
D_3	Moderate	significant structural and non-structural damage	24	[0.90-2.70]
D_4	Severe	irreparable structural damage, will require demolition	21	[0.96-3.07]
D_5	Collapse	complete structural collapse	40	[1.00-5.35]
			N_{CL} = 120	

* [*min-max*] values (in meters) associated with each damage state.

3.2 Case Study 2: The 2018 Sulawesi-Palu Tsunami

On Friday 28 September 2018, at 18:02 p.m. local time, a shallow strike-slip earthquake of moment magnitude 7.5 occurred near Palu City, Central Sulawesi, Indonesia followed by submarine landslides, a tsunami, and massive liquefaction caused substantial damage (Muhari et al. 2018, Rafliana et al. 2022). In Sulawesi, more than 3300 fatalities and missing people, 4400 serious injuries and 170,000

people were displaced by earthquake, tsunami, landslides, liquefaction or building collapse, or
combinations of these hazards (Paulik et al. 2019, Mas et al. 2020). Herein, the damage data related to
the non-engineered unreinforced clay brick masonry buildings (1 & 2 storey) and non-engineered light
timber buildings locaed in Palu City were utilized. Based on the observed damage (see Paulik et al.
2018 for more details on damage observation), each structure was assigned a damage state between
(DS_0 and DS_3). The original data reporting the tsunami flow depth and the attributed damage state to
each surveyed building can be found as supplementary material to Paulik et al. (2018). The three
damage stateslevels ($N_{DS} = 3$) and a description of the indicators leading to the classification of the
damage state are given in Table 2 based.

Table 2. The classification of damage thresholds (the damage scale) used for 2018 Sulawesi Palu Tsunami (from Paulik et al. 2018).

Damage Level	Damage level description	
D_0	None	no damage
D_1	Repairable	partial damage, repairable
D_2	Unrepairable	partial damage, unrepairable
D_3	Complete	complete structural collapse

3.3 The building classes

Damage Level	Damage level description	
D_0	None	no damage
D_1	Repairable	Partial damage, repairable
D_2	Unrepairable	Partial damage, unrepairable
D_3	Complete	Complete structural collapse

The building classes

Table 3 illustrates the building classes, for which fragility curves are obtained based on the proposed
procedure, and based on the two databases related to the two Tsunami events described above. The
taxonomy used for describing the building class matches the original description used in the raw
databases. The number of data points available for different building classes showcases both classes
with large number of data available, e.g., (e.g., brick masonry 1 storey / (South Pacifiec) and non-
engineered brick masonry 1 storey /(Sulawesi), and classes with few data points available (, e.g., timber
residential / (South Pacific) and non-engineered masonry 2 storeys and Timber / (Sulawesi). The
fourthfifth column in the table shows the number of the proportion of the number of damage levels for
calculating the empirical damage levelsfragility curves which observed data is available N for which
observed damage data are available (see Section 2.1) to the total number of damage levels in the
corresponding damage scales, namely $N_{DS}+1==6$5 for South Pacific and $N_{DS}+1==4$3 for Sulawesi
tsunami events (to include level 0). If the ratio is equal to unity, it indicates that data is available for all
the damage levels from 0 to N_{DS}. Note that the number of fragility curves derived is going to be equal

to N-1, that is, equal to the number of damage levels for which observed damage data is available minus one.

Table 3. The buildings cClasses

Class Number	Building Class	Tsunami Event	Number of Data Points	Number of fragility curves, N/N_{DS}
1	Brick masonry residential, 1 storey	South Pacific 2009	120	5/5
2	Timber residential	South Pacific 2009	23	3/5
1	Non engineered masonry, unreinforced with clay brick, 1 storey	Sulawesi-Palu 2018	279	23/3
2	Non engineered masonry, unreinforced with clay brick, 2 storeyesys	Sulawesi-Palu 2018	37	2/3
3	Non engineered light timber	Sulawesi-Palu 2018	14	2/3

355

Table 3. The buildings Classes

	Building Class	Tsunami event	Number of Data	$N/(N_{DS}+1)$, index
1	Brick masonry residential, 1 storey	South Pacific 2009	120	6~~5~~/65, index = {0,~~0,~~1,2,3,4,5}
2	Timber residential	South Pacific 2009	23	4~~3~~/65, index = {2,3,4,5}
1	Non engineered masonry, unreinforced with clay brick, 1 storey	Sulawesi-Palu 2018	279	3~~2~~/43, index = {0,~~0,~~1,2}
2	Non engineered masonry, unreinforced with clay brick, 2 storeys	Sulawesi-Palu 2018	37	3~~2~~/43, index = {0,~~0,~~1,2}
3	Non engineered light timber	Sulawesi-Palu 2018	14	3~~2~~/43, index = {1,2,3}

360 *The fourth column in Table 1 illustrates the distribution of data for masonry residential building class surveyed based on the observed damage level ($n_{CL,j}$, $j = 0:N_{DS}$, with the total sum of $N_{CL} = 120$ buildings surveyed for this class). The last column shows the range of the flow depth associated with each damage state.*

~~5.3~~3.4 The different model classes

365 For each building class considered, w~~W~~e have considered the set of candidate models consisting of the fragility models resulting from the three alternative link functions used in the generalized linear regression in Equation (5). That is, $\mathbb{M}_1$ refers to hierarchical fragility modelling based on "~~probit~~logit"; $\mathbb{M}_2$ refers to hierarchical fragility modelling based on "~~logit~~probit"; $\mathbb{M}_3$ refers to hierarchical fragility modelling based on "cloglog". For each model, both the MLE method using the MATLAB generalized
370 regression toolbox and the ~~Bayesian inference~~BMCS using the procedure described in the previous section are implemented.

~~5.4~~3.5 Fragility modelling using MLE

The first step towards ~~calculating the fragilities~~direct fragility assessment ~~(FA)~~ by employing the MLE method (see Section 2.3) is to define the vector of model parameters $\boldsymbol{\theta} = \{\alpha_{0,j}, \alpha_{1,j}\}$, where $j =$
375 $\mathbf{index}(1:(N-1))$ ~~(j'):$N_{DS} - 1 = 4$, where $j' = 1:N - 1$, index~~ is def~~where vector~~ **index** is defined in Section 2.1 as the vector of damage level indices (in ascending order) for which observed damage data is available and N is length of **index**. ~~To accomplish this, ~~the jth~~ pair of~~ the model parameters

$\{\alpha_{0,j}, \alpha_{1,j}\}$ are obtained by fitting the link functions in Equation (5) to conditional fragility $P(D \geq D_{j+1}|D \geq D_j, IM)$ according to Equation (6). Herein, we have used MATLAB as a statistical software package (developed by MathWorks) to estimate the maximum likelihood of model parameters $\{\alpha_{0,j}, \alpha_{1,j}\}$ using the following MATLAB command: glmfit(log($\mathbf{x}_j$), $\mathbf{y}_j$, 'binomial', 'link', 'model'). The 'model' will be either 'logit', 'probit', or 'comploglog'. For each damage level D_{j+1}, $\mathbf{index}(1) \leq j < \mathbf{index}(N)$, the vector $\mathbf{x}_j$ is the IM's for which the condition $D \geq D_j$ is satisfied; $\mathbf{y}_j$ is the column vector containing one-to-one probability assignment to the IM data in $\mathbf{x}_j$ with zero (=0.0) assigned to those data corresponding to DS_j ($D_j \leq D < D_{j+1}$) and one (=1.0) to those related to higher damage states (with $D \geq D_{j+1}$).

The vectors defining the MLE of the model parameters, $\boldsymbol{\theta}_{MLE}$, are presented in Table 4 for each of the building classes listed in Table 3 and for each of the three models $\mathbb{M}_1$, $\mathbb{M}_2$, and $\mathbb{M}_3$ defined in Section 3.4. Given the model parameter $\boldsymbol{\theta}_{MLE}$, the damage state probability $P(DS_j|IM)$ can be estimated based on the recursive Equation (7) and Equation (8). Then, the fragility for the ultimate damage level $D_{\mathbf{index}(N)}$, i.e., $P(D \geq D_5|IM, \boldsymbol{\theta}_{MLE})$, is calculated first based on Equation (8). For the lower damage thresholds D_j, where $0 < j < 5$, the empirical fragility $P(D \geq D_j|IM, \boldsymbol{\theta}_{MLE})$ is derived based on the Equation (9). The resulting hierarchical fragility curves by employing the direct fragility assessment given $\boldsymbol{\theta}_{MLE}$, i.e., $P(D \geq D_j|IM, \boldsymbol{\theta}_{MLE})$ for $j = \mathbf{index}(2):N+1$, are shown later in the next section by comparison with those obtained from the BMCS method.

Table 4. The model parameters $\boldsymbol{\theta}_{MLE}$.

	Building Class	Model Class	$\alpha_{0,0}$	$\alpha_{1,0}$	$\alpha_{0,1}$	$\alpha_{1,1}$	$\alpha_{0,2}$	$\alpha_{1,2}$	$\alpha_{0,3}$	$\alpha_{1,3}$	$\alpha_{0,4}$	$\alpha_{1,4}$
South Pacific Tsunami 2009	1	$\mathbb{M}_1$	5.242	4.190	3.900	4.255	-1.175	4.805	-1.345	2.887	-1.994	2.917
		$\mathbb{M}_2$	2.742	2.190	2.007	2.221	-0.670	2.804	-0.803	1.745	-1.157	1.733
		$\mathbb{M}_3$	2.079	2.011	1.322	1.850	-1.268	3.057	-1.366	1.961	-1.981	2.218
	2	$\mathbb{M}_1$					1.127	1.512	2.484	0.771	-2.846	2.708
		$\mathbb{M}_2$					0.657	0.909	1.390	0.426	-1.575	1.316
		$\mathbb{M}_3$					0.251	0.862	0.883	0.355	-2.141	1.648
Sulawesi-Palu Tsunami 2018	1	$\mathbb{M}_1$	6.059	4.355	-0.630	2.909						
		$\mathbb{M}_2$	3.264	2.340	-0.371	1.709						
		$\mathbb{M}_3$	2.498	2.088	-0.907	2.056						
	2	$\mathbb{M}_1$	3.556	3.672	-2.486	5.126						
		$\mathbb{M}_2$	2.077	2.144	-1.464	3.036						
		$\mathbb{M}_3$	1.664	2.239	-2.451	4.217						
	3	$\mathbb{M}_1$			0.466	1.375	0.474	1.195				
		$\mathbb{M}_2$			0.295	0.847	0.296	0.774				
		$\mathbb{M}_3$			-0.041	1.068	-0.076	0.835				

Table 4. The model parameters $\boldsymbol{\theta}_{MLE}$.

Model	$\alpha_{0,0}$	$\alpha_{1,0}$	$\alpha_{0,1}$	$\alpha_{1,1}$	$\alpha_{0,2}$	$\alpha_{1,2}$	$\alpha_{0,3}$	$\alpha_{1,3}$	$\alpha_{0,4}$	$\alpha_{1,4}$
$\mathbb{M}_1$	5.242	4.190	3.900	4.255	-1.175	4.805	-1.345	2.887	-1.994	2.917

M₂	2.742	2.190	2.007	2.221	-0.670	2.804	-0.803	1.745	-1.157	1.733
M₃	2.079	2.011	1.322	1.850	-1.268	3.057	-1.366	1.961	-1.981	2.218

5.56~3.6 Fragility modelling using BMCS

In the first step, the model parameters are estimated for each model class separately. For each model class $\mathbb{M}_k$, the $2NN_{DS} = 10$ model parameters $\boldsymbol{\theta}_k$ are estimated through the adaptive MCMC method described in detail in Appendix E which yields the posterior distribution in Equation (14). With reference to Equation (14), the prior joint PDF $p(\boldsymbol{\theta}_k|\mathbb{M}_k)$ should be assigned in advance. As noted previously, $p(\boldsymbol{\theta}_k|\mathbb{M}_k)$ can~is be a multivariate normal PDF with zero correlation between the pairs of model parameters $\boldsymbol{\theta}_{10\times1}$ (see Appendix D). The vector of the mean values, $\boldsymbol{\mu}_{\boldsymbol{\theta}}$ $\boldsymbol{\mu}_{\boldsymbol{\theta}_{10\times1}}$, is set to be the MLE tabulated in Table 2 (= $\boldsymbol{\theta}_{MLE}$ related to $\mathbb{M}_k$). We have attributed a high value for the coefficient of variation (COV=more than 1.60~3.20 herein) for each of the 10 model parameters. Appendix F illustrates the histograms representing the drawn samples from the joint posterior PDF $p(\boldsymbol{\theta}_k|\mathbf{D},\mathbb{M}_k)$ for a selected each of the 10 model parameters and five building classes in Table 3. The marginal normal prior PDFs are also shown (with statistics defined previously).

The robust fragility (RF) curves derived from the hierarchical fragility curves (see Section 2.5) and the corresponding ± plus/minus two one standard deviation ($\pm 1\sigma$) intervals from Equation (16) and Equation (17) are also plotted in Figure 2a to Figure 6~4a corresponding to C~Classes 1-2 South Pacific Tsunami and Classes 1-3 Sulawesi-Palu $\mathbb{M}_1$ to $\mathbb{M}_3$, for one of the model classes $\mathbb{M}_k$ ($k \in \{1,2,3\}$) and for the damage thresholds D_1-D_j, $j = \mathbf{index}(2~2:N+1)$ to D_{N5}. The colors of the hierarchical robust fragility RF curves, labled as D_j-BMCS, match closely those shown in Figure 1~Tables 1 and 2. The corresponding $\pm 1\sigma$ ± two standard deviation confidence interval curve, which reflects the uncertainty in the model parameters, is shown as a light grey area with different color intensities. Figures 2b to Figure 6~4b compare the hierarchical robust fragility~RF and its confidence interval, labeled as D_j-BMCS, with the result of the direct fragility assessment hierarchical fragility assessment based on maximum likelihood estimation(FA, (see MLE method in~previous Section Section 2.3~3.5), labeled as D_j-MLE, for $1 \le j \le N5$. The MLE-based~fragility FA curves are shown with similar colors (and darker intensity) and with the same line type (and half of the thickness) of the corresponding robust fragility~RF curves. The first observation is that the results of MLE-based fragilities and the BMCS-based fragilities are quite close in all damage thresholds (as expected, see Jalayer and Erahimian 2020). Moreover, the BMCS provides also the confidence bands for the fragility curves, which cannot be directly provided by the MLE method. To showcase an individual fragility curve, Figure 2c to Figure 6~4c illustrate the empirical fragility curves associated with the lth realization of the vector of model parameters $\boldsymbol{\theta}_{k,l}$ for model class $\mathbb{M}_k$ (where l is defined on each figure separately), i.e., $P(D \ge D_j|IM,\boldsymbol{\theta}_{k,l})$ where $1 \le j \le N5$ (see Section 2.5). Figures 2d to Figure 6~4d illustrate the robust fragility~RF curve associated with the ultimate damage threshold $D_{\mathbf{index}(N)}$ D_{N5}, together with all the N_d~sample fragilities (N_d=903 for $\mathbb{M}_1$, N_d=882 for $\mathbb{M}_2$, and N_d=951 for $\mathbb{M}_3$) shown with thin gray lines. N_d is the number of distinct samples as discussed in Appendix E and Appendix F of this manuscript. The intensity values for which the damage level is not exceeded are shown with blue circles having the probability equal to zero. Other IMs that lead to the exceedance of the damage level are shown with red circles with a probability equal to one. The total number of samples generated by adaptive MCMC in its last chain is N_{seed}=1000 ($N_d \le N_{seed}$). Figure 2d to 6~4d also illustrate all the fragility parameters described in Section 2.5 including the equivalent lognormal parameters η_{IM_C} and β_{IM_C}, the epistemic uncertainty in the empirical fragility assessment β_{UF}, and also the intensities IM_C^{16}, IM_C^{84}, IM^{84} and, and IM^{16} a (the latter two are s~IM values at the median (, i.e. 50% probability.) from the RF minus/plus one standard deviation, respectively (see Section 2.5). For all 5 buildings classes considered (ie, two classes for South Pacific

Table 3. The equivalent lognormal parameters and the epistemic uncertainty in the RF assessment for damage thresholds D_1 to D_5 and for the model classes $\mathbb{M}_1$ to $\mathbb{M}_3$

Damage threshold	Model 1 ($\mathbb{M}_1$)			Model 2 ($\mathbb{M}_2$)			Model 3 ($\mathbb{M}_3$)		
	η_{IM_C}[m]	β_{IM_C}	β_{UF}	η_{IM_C}[m]	β_{IM_C}	β_{UF}	η_{IM_C}[m]	β_{IM_C}	β_{UF}
D_1	0.29	0.42	0.21	0.30	0.45	0.21	0.33	0.52	0.21
D_2	0.44	0.34	0.14	0.45	0.38	0.15	0.49	0.40	0.15
D_3	1.29	0.35	0.07	1.27	0.35	0.07	1.37	0.37	0.07
D_4	1.82	0.42	0.06	1.79	0.44	0.06	1.90	0.37	0.06
D_5	2.49	0.46	0.07	2.46	0.45	0.07	2.51	0.34	0.06
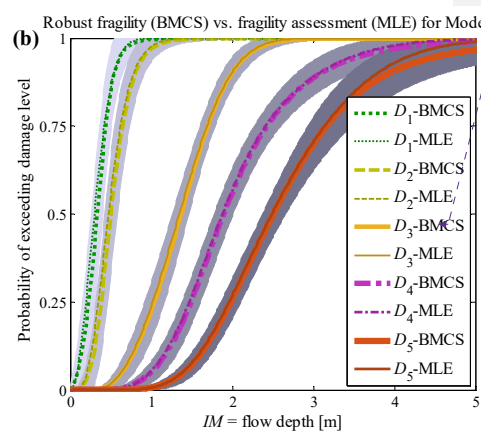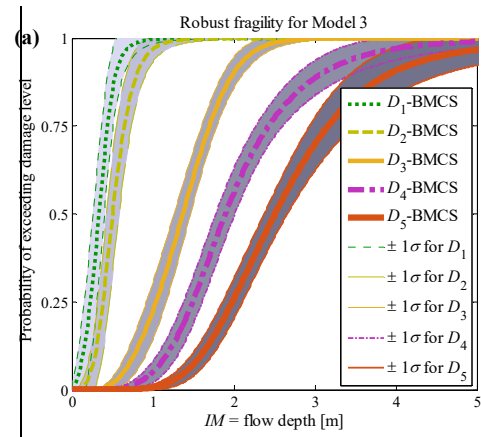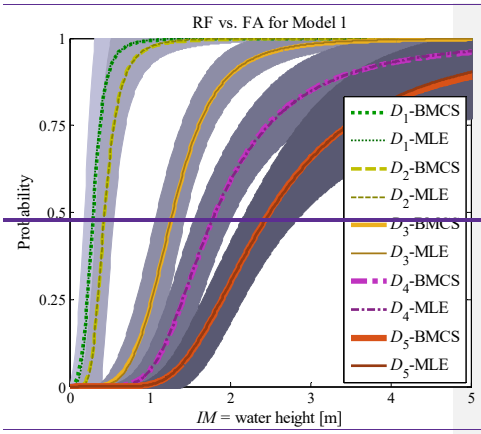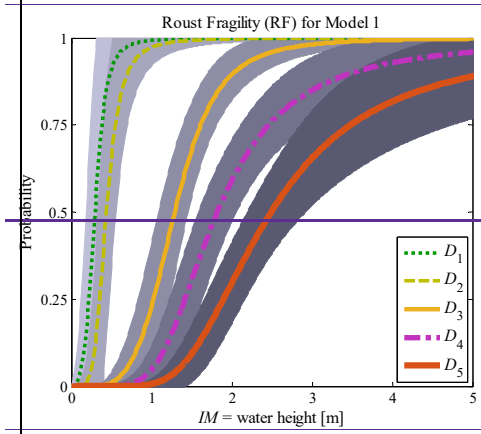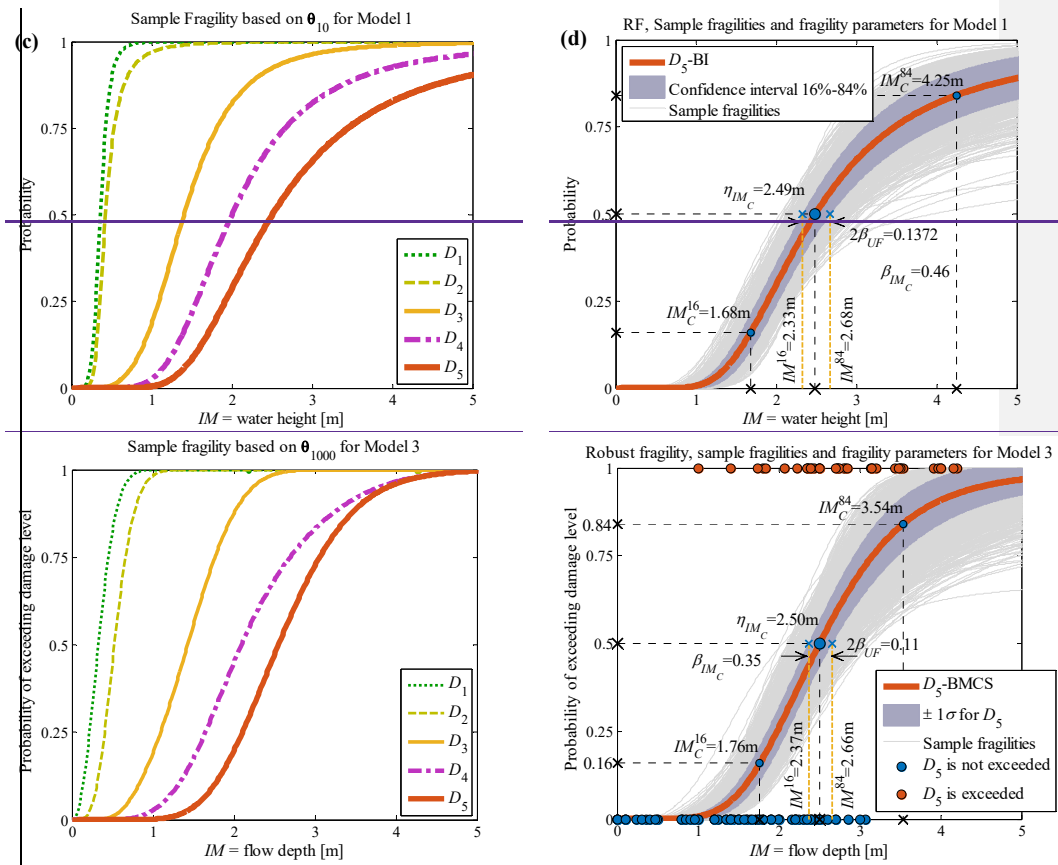
Figure 2: Building class 1 (brick masonry residential, 1 storey) of South Pacific 2009 Tsunami considering fragility Model class $\mathbb{M}_{13}$: (a) Hierarchical rRobust fragility curves (RF) and their ± two standard deviation confidence intervals; (b) comparison between hierarchical robust fragility curvesRF and theirits confidence band (based on BMCS method) and fragility assessment FA (based on MLE method); (c) the fragility curves $P\left(D \geq D_j \middle| IM, \theta_{13,1000}\right)$ where $1 \leq j \leq 5$ associated with the 1000th realization of the model parameters, $\theta_{13,1000}$ ($k=1\ 3$ associated to model $\mathbb{M}_{13}$, $l=1000$); (d) RF associated with the damage threshold D_5, together with all the $N_s=903$ sample fragilities, and the equivalent lognormal fragility parameters.

470
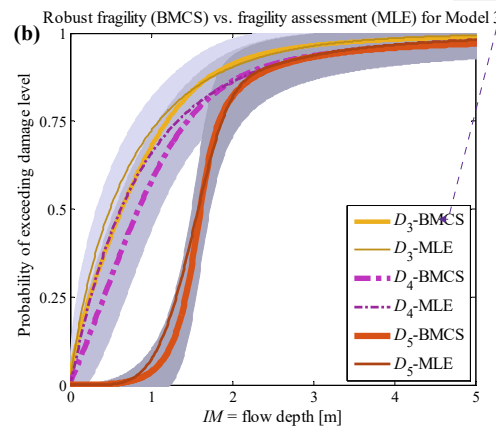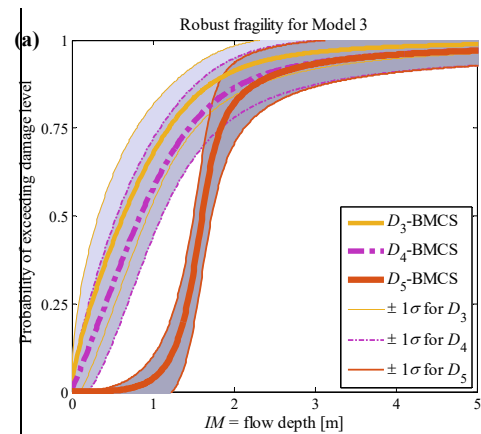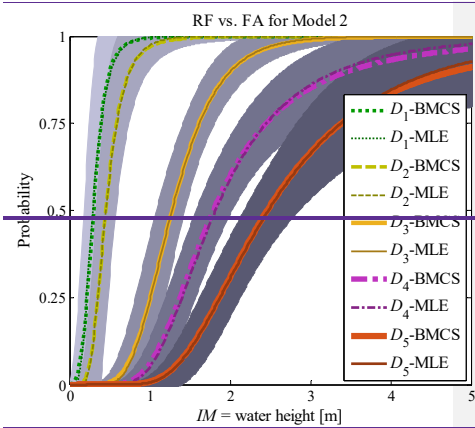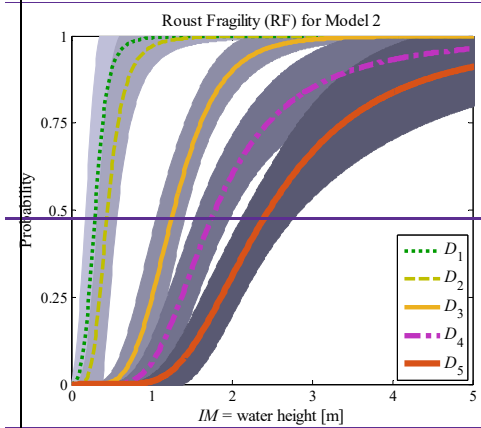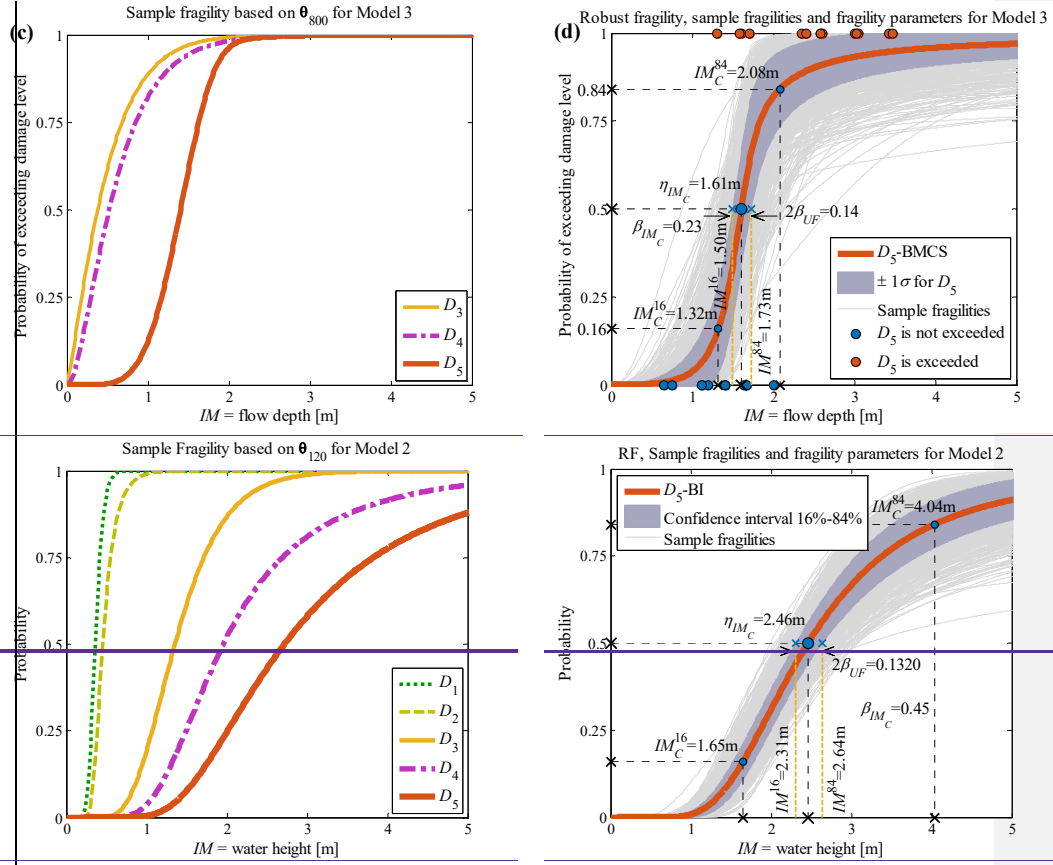
475 **Figure 3:** **Building class 2 (Timber residential) of South Pacific 2009 Tsunami considering fragility Model class $\mathbb{M}_3$** Model class $\mathbb{M}_2$ **(a)** **Hierarchical r**obust fragility curves ~~(RF)~~ and their ± two standard deviation confidence intervals; **(b)** comparison between **hierarchical robust fragility curves** ~~RF~~ and **their** ~~its~~ confidence band (based on BMCS method) and **fragility assessment** ~~FA~~ (based on MLE method); **(c)** the fragility curves $P(D \ge D_j | IM, \theta_{23,120800})$ where ~~13~~ $\le j \le 5$ associated with the ~~120th~~ **800th** realization of 480 the model parameters, $\theta_{23,80120}$ (k=~~2~~ **3** associated to model $\mathbb{M}_{23}$, l=~~120~~**800**); **(d)** **R**obust fragility ~~F~~ associated with the damage threshold D_5, together with all the ~~N_s=882~~ sample fragilities, and the equivalent lognormal fragility parameters.
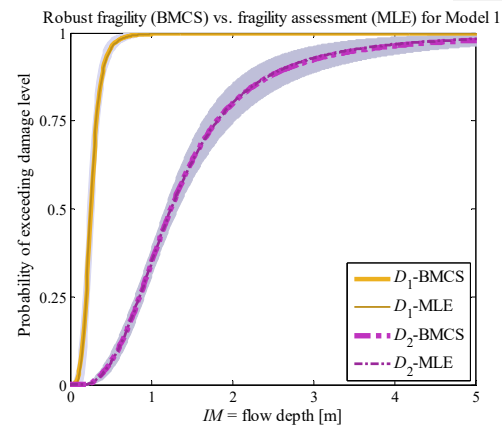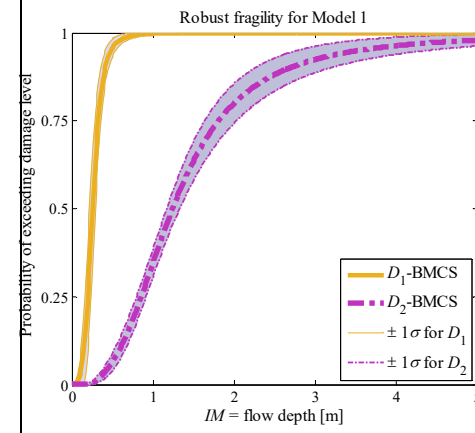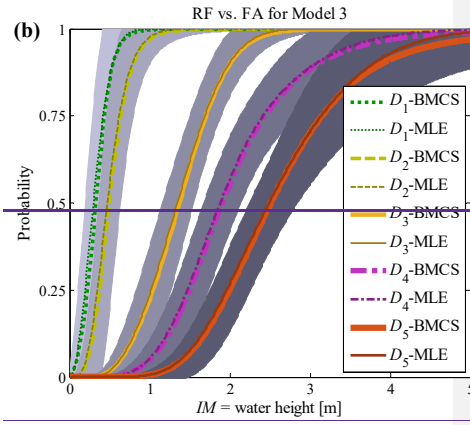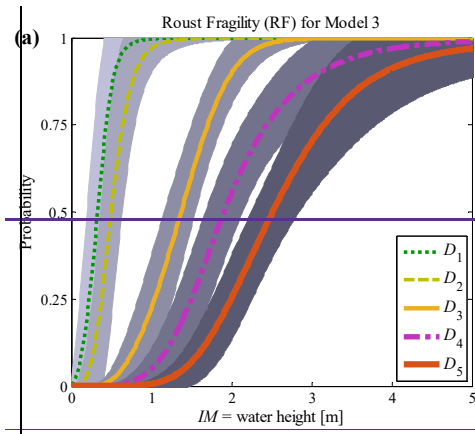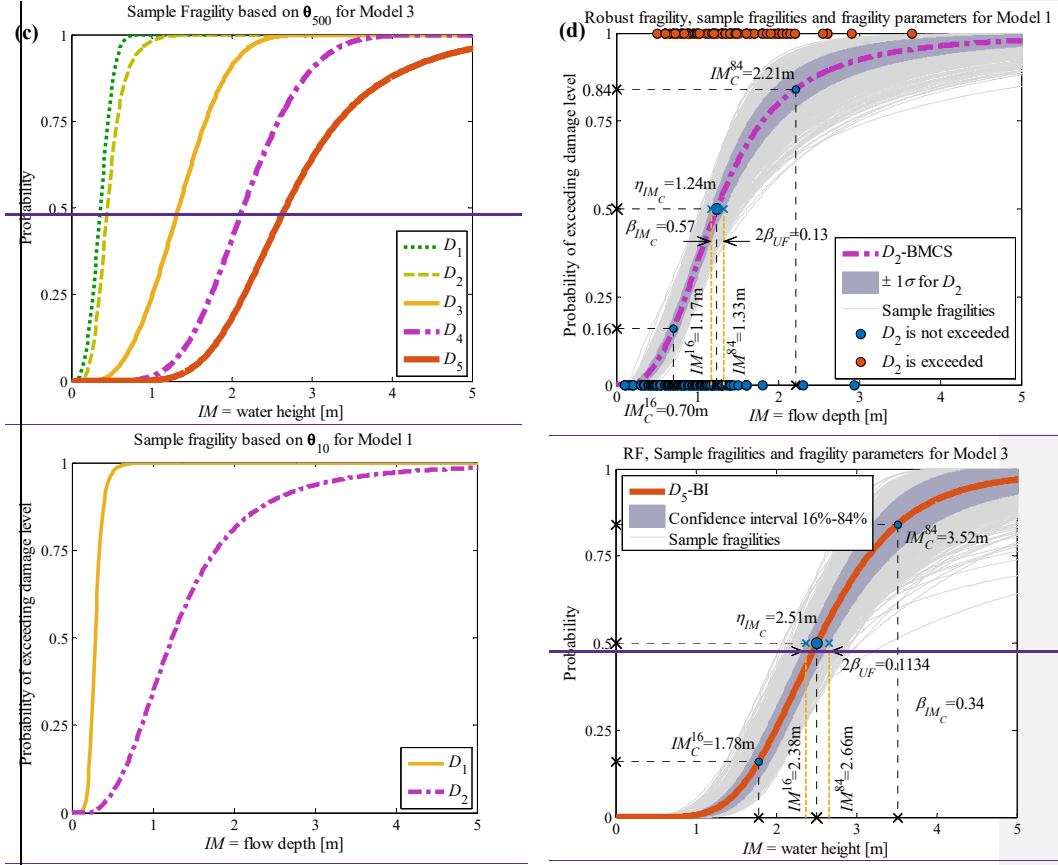
Figure 4: Building class 1 (Non engineered masonry, unreinforced with clay brick, 1 storey) of Sulawesi-Palu 2018 Tsunami considering fragility Model class~~Model class~~ $\mathbb{M}_{31}$ **(a)** Robust fragility curves (RF) and their ± two standard deviation confidence intervals; **(b)** comparison between hierarchical robust fragility RF and its confidence band (based on BMCS method) and fragility assessment~~FA~~ (based on MLE method~~)~~; **(c)** the fragility curves $P(D \geq D_j | IM, \theta_{31,5010})$ where $1 \leq j \leq$ ~~5~~2 associated with the ~~500th~~10th realization of the model parameters, $\theta_{31,5010}$ (k=~~3~~1 associated to model $\mathbb{M}_{31}$, l=~~500~~10); **(d)** Robust fragility curve~~F~~ associated with the damage threshold ~~D_5~~D_2, together with all the ~~N_{sf}=951~~ sample fragilities, and the equivalent lognormal fragility parameters.
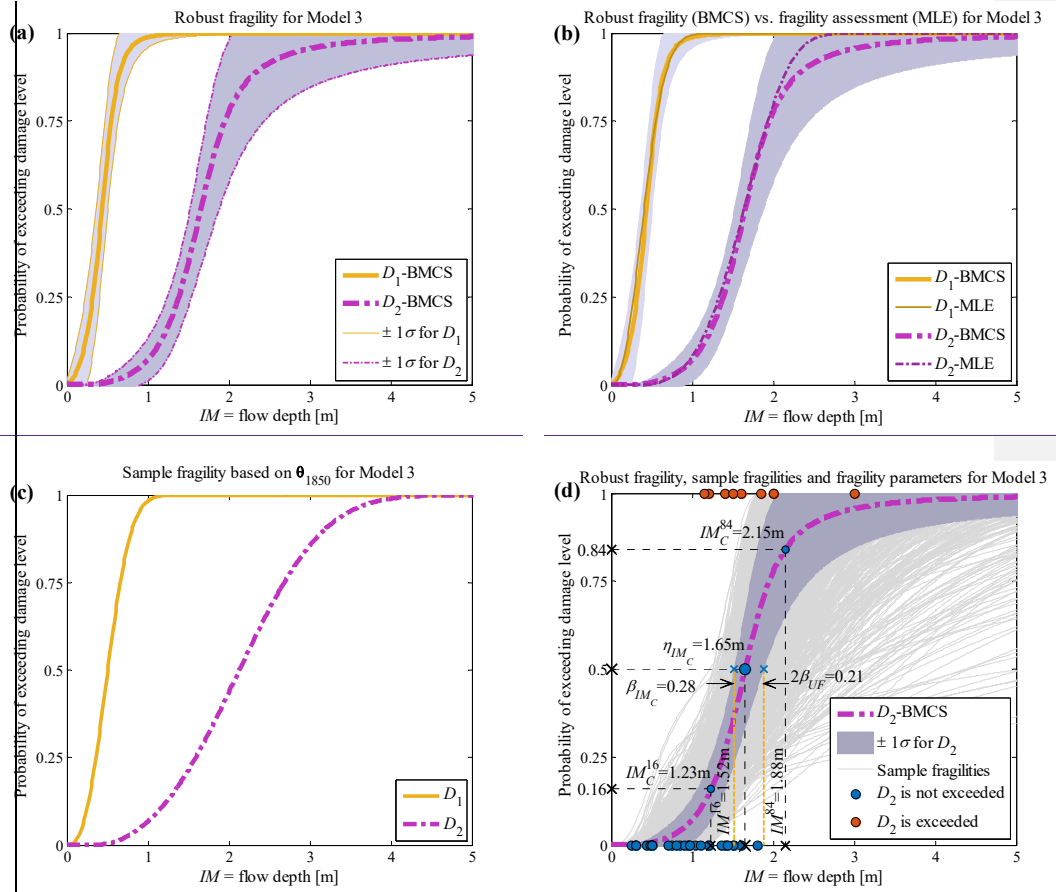
Figure 5: Building class 2 (Non engineered masonry, unreinforced with clay brick, 2 storey) of Sulawesi-Palu 2018 Tsunami considering fragility Model class $\mathbb{M}_3$ (a) Hierarchical r̶Robust fragility curves (RF) and their ± two standard deviation confidence intervals; (b) comparison between robust fragility ̶RF and its confidence band (based on BMCS method) and fragility assessment ̶FA (based on MLE method); (c) the fragility curves $P(D \geq D_j | IM, \theta_{3,1850})$ where $1 \leq j \leq 2$ associated with the 1850th realization of the model parameters, $\theta_{3,1850}$ (k=3 associated to model $\mathbb{M}_3$, l=1850); (d) R̶obust fragility curve̶F associated with the damage threshold D_2, together with all the sample fragilities, and the equivalent lognormal fragility parameters.

Formattato: New paragraph, Interlinea: multipla 1.15 ri
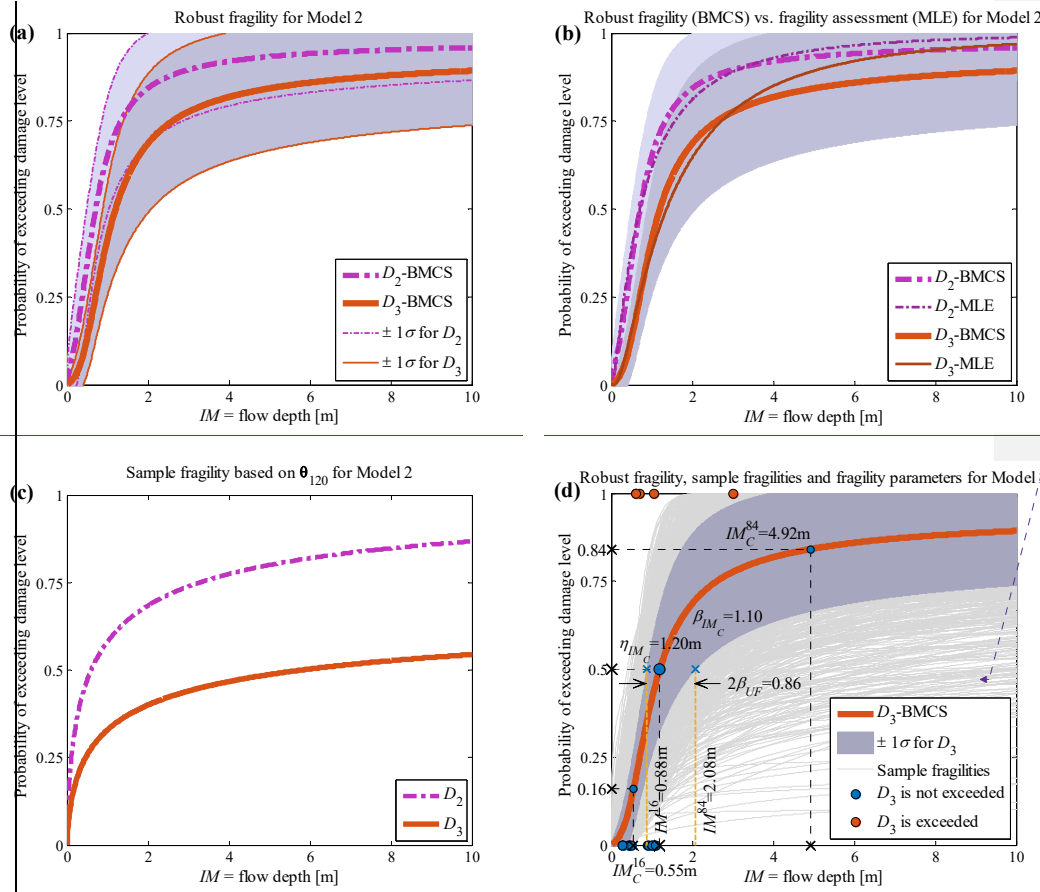
Figure 6: Building class 3 (Non engineered light timber) of Sulawesi-Palu 2018 Tsunami considering fragility Model class $\mathbb{M}_2$ (a) Hierarchical rRobust fragility curves (RF) and their ± two standard deviation confidence intervals; (b) comparison between robust fragilityRF and its confidence band (based on BMCS method) and fragility assessment FA (based on MLE method); (c) the fragility curves $P(D \geq D_j | IM, \theta_{2,120})$ where $2 \leq j \leq 3$ associated with the 120th realization of the model parameters, $\theta_{2,120}$ (k=2 associated to model $\mathbb{M}_2$, l=120); (d) Robust fragility curveF associated with the damage threshold D_3, together with all the sample fragilities, and the equivalent lognormal fragility parameters.

Table 3. The equivalent lognormal parameters and the epistemic uncertainty in the RF assessment for all the building classes, damage thresholds, and model classes $\mathbb{M}_1$ to $\mathbb{M}_3$

	Building Class	Damage Levelthreshold	Model 1 ($\mathbb{M}_1$)			Model 2 ($\mathbb{M}_2$)			Model 3 ($\mathbb{M}_3$)		
			η_{IM_C}[m]	β_{IM_C}	β_{UF}	η_{IM_C}[m]	β_{IM_C}	β_{UF}	η_{IM_C}[m]	β_{IM_C}	β_{UF}
South Pacific Tsunami 2009	1	D_1	0.29	0.40	0.20	0.30	0.46	0.22	0.33	0.51	0.22
		D_2	0.43	0.35	0.15	0.46	0.37	0.15	0.50	0.40	0.15
		D_3	1.28	0.35	0.08	1.28	0.35	0.07	1.37	0.37	0.07
		D_4	1.80	0.45	0.07	1.81	0.42	0.07	1.89	0.37	0.06
		D_5	2.49	0.47	0.07	2.48	0.47	0.07	2.50	0.35	0.06
	2	D_3	0.64	1.08	0.58	0.63	1.20	0.64	0.63	1.26	0.53
		D_4	0.73	1.01	0.48	0.75	1.01	0.46	0.84	0.98	0.35
		D_5	1.52	0.25	0.08	1.54	0.26	0.08	1.61	0.23	0.07
Sulawesi-Palu Tsunami 2018	1	D_1	0.25	0.39	0.15	0.26	0.43	0.15	0.27	0.56	0.18
		D_2	1.24	0.57	0.06	1.24	0.59	0.07	1.31	0.58	0.06
	2	D_1	0.39	0.44	0.20	0.38	0.45	0.19	0.43	0.43	0.17
		D_2	1.60	0.31	0.11	1.59	0.32	0.12	1.65	0.28	0.11
	3	D_2	0.74	1.01	0.34	0.71	1.03	0.38	0.81	0.85	0.29
		D_3	1.16	0.98	0.39	1.20	1.10	0.43	1.29	0.95	0.31

515

5.573.7 Model selection

With reference to Equation (12), the *log-evidence* $\ln[p(\mathbf{D}|\mathbb{M}_k)]$, can be estimated by subtracting *Term 2 1from and Term 12*. *Term 1The former* denotes the posterior mean of the log-likelihood, and the *Term 2latter* is the relative entropy between the prior and the posterior. Within the BMCS method, these two terms are readily computable.

520

Given the samples generated from the joint posterior PDF's $\boldsymbol{\theta}_k$, *Term 1* (=*Average Data Fit*) can be seen as the expected value of the log-likelihood over the vector of fragility parameters $\boldsymbol{\theta}_k\boldsymbol{\theta}$ given the model $\mathbb{M}_k$, i.e., $\mathbb{E}_{\boldsymbol{\theta}_k|\mathbf{D},\mathbb{M}_k}(\ln[p(\mathbf{D}|\mathbb{M}_k)])$. *Term 2* (=*Relative EntropyInformation Gain*) is calculated as the expected value of information gain or entropy between the two PDF's posterior and prior over the vector $\boldsymbol{\theta}$ given the model $\mathbb{M}_k$, i.e., $\mathbb{E}_{\boldsymbol{\theta}_k|\mathbf{D},\mathbb{M}_k}(\ln[p(\boldsymbol{\theta}_k\boldsymbol{\theta}|\mathbf{D},\mathbb{M}_k)/p(\boldsymbol{\theta}_k\boldsymbol{\theta}|\mathbb{M}_k)])$. It is noted that based on Jensen's inequality, the mean information gain (relative entropy) of posterior compared to the prior is always non-negative (see e.g., Jalayer et al. 2012, Ebrahimian and Jalayer 2021). Hence, Term 2 should always be positive. Herein, $p(\boldsymbol{\theta}_k\boldsymbol{\theta}|\mathbf{D},\mathbb{M}_k)$ is constructed by an adaptive kernel density function (see

525

Equation E5, Appendix E) as the weighted sum (average) of Gau102*N* dimensional Gaussian PDFs centered among the samples $\boldsymbol{\theta}_k$ given model $\mathbb{M}_k$ (k=1:3). The prior $p(\boldsymbol{\theta}_k\boldsymbol{\theta}|\mathbb{M}_k)$ is a multivariate normal PDF, respectively with the mean and covariance described previously for each model (see Equation D1 in Appendix D). Table 4 shows the results for model class selection for all 5 buildings classes considered. The last column illustrates the posterior probability (weight) of the model $P(\mathbb{M}_k|\mathbf{D})$ according to Equation (10) assuming that the prior $P(\mathbb{M}_k) = \frac{1}{3}$ (where k=1:3). The best model for each building class is shown with a blue color.

530

535

For instance, for Class 1 (masonry residential) for South Pacific Tsunami, Model class $\mathbb{M}_3$ (using a complementary log-log "cloglog" transformation of π_{ij} to the linear logarithmic space, see Equation 5) is preferred, since it has an overall larger difference between data fit and mean information gain, which leads to a higher the log-evidence. The posterior weights (last column of Table 4, see also Equation 10) of 6%, 11% and 83% are stabilized through different runs of the BMCS method with around 2% changes. It should be noted that in Figures 2 to 6, we reported directly the fragility results for the "best"

540

fragility model class (i.e., the one that maximizes log evidence) identified based on the procedure described here.

Table 4. Bayesian model class selection results for empirical fragility models

Building Class		Model Class	*Term* 1: Average Data Fit	*Term* 2: Information Gain	Log-Evidence	Posterior Probability of the model
South Pacific Tsunami 2009	1	$\mathbb{M}_1$	-124.4561 ~~-124.2898~~	23.6853 ~~17.3825~~	-148.6723 ~~-141.1414~~	0.058 ~~055~~
		$\mathbb{M}_2$	-123.4659 ~~-123.1298~~	23.9566 ~~17.9314~~	-147.0612 ~~-141.4224~~	0.107 ~~113~~
		$\mathbb{M}_3$	-120.6454 ~~-120.6051~~	24.7810 ~~18.4015~~	-145.0066 ~~-139.4264~~	0.835 ~~832~~
	2	$\mathbb{M}_1$	-20.4791	9.7549	-30.2340	0.315
		$\mathbb{M}_2$	-19.9106	10.4660	-30.3766	0.273
		$\mathbb{M}_3$	-19.7565	10.2117	-29.9682	0.411
Sulawesi-Palu Tsunami 2018	1	$\mathbb{M}_1$	-161.9565	9.5690	-171.5255	0.445
		$\mathbb{M}_2$	-161.2320	10.5660	-171.7979	0.339
		$\mathbb{M}_3$	-161.8821	10.3673	-172.2494	0.216
	2	$\mathbb{M}_1$	-23.3696	6.8292	-30.1987	0.213
		$\mathbb{M}_2$	-22.7429	7.2697	-30.0126	0.257
		$\mathbb{M}_3$	-22.4307	6.8551	-29.2858	0.531
	3	$\mathbb{M}_1$	-15.8034	4.2741	-20.0775	0.210
		$\mathbb{M}_2$	-15.1575	3.9226	-19.0802	0.570
		$\mathbb{M}_3$	-14.6294	5.4015	-20.0309	0.220

~~For instance, for Class 1 (masonry residential) for South Pacific Tsunami, Model class $\mathbb{M}_3$ (using a complementary log-log "cloglog" transformation of π_{ij} to the linear logarithmic space, see Equation 5) is preferred, since it has an overall larger difference between better data fit and mean information gain, which makes leads to a higher the log-evidence greater. In terms of the information gain, all the three models perform similarly with higher value attributed to $\mathbb{M}_3$ (and obviously being more penalized for it). After $\mathbb{M}_3$, the model $\mathbb{M}_2$ with a lognormal distribution ("probit") is preferred compared to $\mathbb{M}_1$ with a logistic regression model ("logit") It is noteworthy that as new samples $\boldsymbol{\theta}_k$ become available through the BMCS method by performing new MCMC sampling, the posterior model probabilities will change; however, the whole procedure seems to be stable; i.e., the evidence that $\mathbb{M}_3$ is preferable among the models using the BMCS holds. The posterior weights (last column of Table 4, see also Equation 10) of 6%, 11% and 83% are s is stabilized through different runs of the BMCS method with around 2% changes. It is noted that based on Jensen's inequality, the mean information gain of posterior compared to the prior is always non-negative (see e.g., Jalayer et al. 2012). Hence, Term 2 should always be positive.It should be noted that in Figures 2 to 6, we reported directly the fragility results for the "best" fragility model class (i.e., the one that maximizes log evidence) identified based on the procedure described here.~~

~~5.58~~3.8 The "Basic" (MLE-basic) method: fitting data to one damage state at a time

In the ~~traditional~~ Basic method (see Section 2.2), the fragility $P(D \geq D_j | IM)$ is obtained by using a generalized linear regression model according to Equation (5) with "logit", "probit" or "cloglog" link function fitted to the damage data ($\mathbb{M}_k$ where $k = 1:3$). With reference to the MLE method described

previously, the vector $\mathbf{x}_j$ herein is the *IM* associated to all damage data (and not partial, as in the hierarchical fragility method described in Section 3.3), and $\mathbf{y}_j$ is the column vector of one-to-one probability assignment to the *IM* data in $\mathbf{x}_j$ with zero (=0) assigned to those data with an observed damage threshold $D < D_j$, and one (=1) to those with $D \geq D_j$. Thus, for the empirical fragility associated with the damage threshold D_j, and based on the model $\mathbb{M}_k$, there are two model parameters to be defined, namely $\boldsymbol{\theta}_{\text{MLE}-Basic} = \{\alpha_0, \alpha_1\}_k$. As noted previously, there might be conditions (depending on the quantity of the observed damage data), where a part of the fragility of damage threshold D_j lies below the fragility of the higher damage level D_{j+1}, indicating that $P(DS_j|IM) < 0$. This is due to the fact that in the traditional method, there is no explicit requirement to satisfy $P(DS_j|IM) > 0$ as compared to the proposed method. The MLE of model parameters $\{\alpha_0, \alpha_1\}$ for the damage levels D_j, $j = \overline{j = \text{index}(2\cancel{2}: N+1)}$ associated with the building classes in Table 3 ~~for damage levels D_1 to D_5 D_N~~ are presented in Table 5.

Figure ~~5~~7 compares the fragility assessment obtained based on MLE-based hierarchical fragility modeling (see also the MLE-based curves in Figure 2b to Figure 6 4b) with the result of fragility assessment~~FA~~ by employing the MLE-*Basic* method for ~~the~~ the "best" ~~ree considered~~ Model Class~~es~~ $\mathbb{M}_k$ ($k \in \{1,2,3\}$ ~~k=1:3~~) identified according to the procedure outlined in the previous section. It is noted that the fragility function~~al form~~ is different between the two methods. MLE-based fragility assessment~~FA~~ given $\mathbb{M}_k$ uses Equation (7) to Equation (9) to construct hierarchical fragility curve given that the conditional fragility term $\pi_{ij} = P(D \geq D_{j+1}|D \geq D_j, IM_i)$, $j = \text{index}(1: N-1)$ has one of the functional forms in Equation (5). However, the fragility assessment~~FA~~ using MLE-*Basic* method employs directly one of the expressions in Equation (5) (corresponding to $\mathbb{M}_k$, k=1:3) to derive the fragility curve $\pi_{ij} = P(D \geq D_j|IM_i)$ (based on the whole damage data) and $j = \text{index}(2: N)$. This difference manifests itself in Figure 7a (for brick masonry residential, Class 1, South Pacific Tsunami) the deviation between the two fragility models ~~in Figure 5, especially~~ for higher damage thresholds D_4 and D_5. The deviations between the fragility curves are particularly noticeable at higher *IM* values (with exceedance probability >50%); however, their medians are quite similar. In 7b for (Timber residential buildings, Class 2 South Pacific Tsunami) and 7e (Light informal timber buildings, Class 3, Sulawesi-Palu tsunami), we can observe that fragility curves intersect in the case of MLE-*Basic* fragility assessment. However, they do not intersect for hierarchical fragility curves. ~~Strictly speaking, the fragilities are closer in the case of $\mathbb{M}_2$ and $\mathbb{M}_3$.~~

The intersection points of the consequent damage states D_{j+1} with D_j ~~due~~when using ~~t~~to the MLE-*Basic* fragility estimation method are shown with color stars on each figure.

Table 5. The Model parameters $\boldsymbol{\theta}_{\text{MLE}-Basic}$.

Building Class	Model Class	$D \geq D_1$		$D \geq D_2$		$D \geq D_3$		$D \geq D_4$		$D \geq D_5$	
		α_0	α_1	α_0	α_1	α_0	α_1	α_0	α_1	α_0	α_1
1	$\mathbb{M}_1$	5.242	4.190	3.655	4.556	-1.221	4.884	-2.666	~~4~~2.213	-4.271	~~4.65~~12
	$\mathbb{M}_2$	2.742	2.190	1.946	2.486	-0.695	2.846	-1.506	2.425	-2.293	2.515

	$\mathbb{M}_3$	2.079	2.011	1.347	2.361	-1.319	3.139	-2.3903 89	3.009	-3.919	3.806
2	$\mathbb{M}_1$					1.127	1.512	0.813	1.392	-2.931	6.055
	$\mathbb{M}_2$					0.657	0.909	0.472	0.873	-1.747	3.597
	$\mathbb{M}_3$					0.251	0.862	0.051	0.914	-2.416	3.922

		$D \geq D_1$		$D \geq D_2$		$D \geq D_3$	
		α_0	α_1	α_0	α_1	α_0	α_1
1	$\mathbb{M}_1$	6.059	4.355	-0.638	2.948		
	$\mathbb{M}_2$	3.264	2.340	-0.375	1.728		
	$\mathbb{M}_3$	2.498	2.088	-0.918	2.088		
2	$\mathbb{M}_1$	3.556	3.672	-2.500	5.160		
	$\mathbb{M}_2$	2.077	2.144	-1.465	3.039		
	$\mathbb{M}_3$	1.664	2.239	-2.473	4.268		
3	$\mathbb{M}_1$			0.466	1.375	-0.501	1.843
	$\mathbb{M}_2$			0.295	0.847	-0.286	1.141
	$\mathbb{M}_3$			-0.041	1.068	-0.787	1.565

South Pacific Tsunami 2009

Tabella formattata

610

615

620

625

630

635
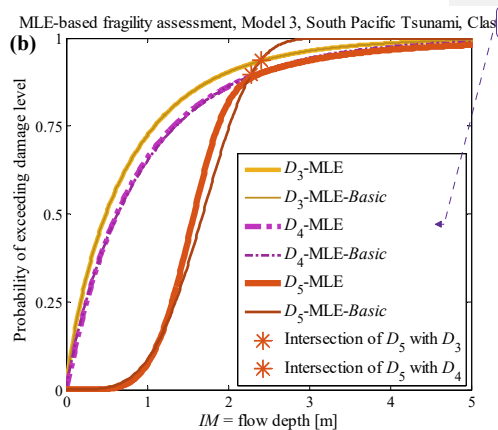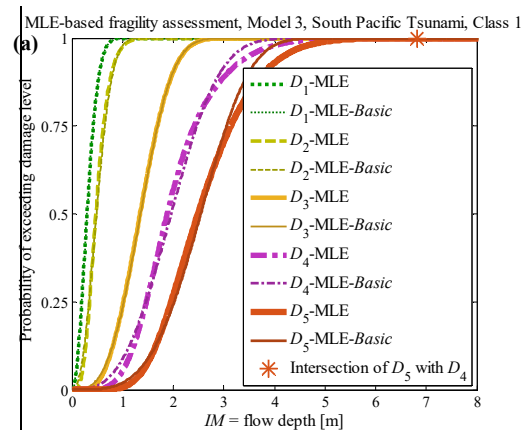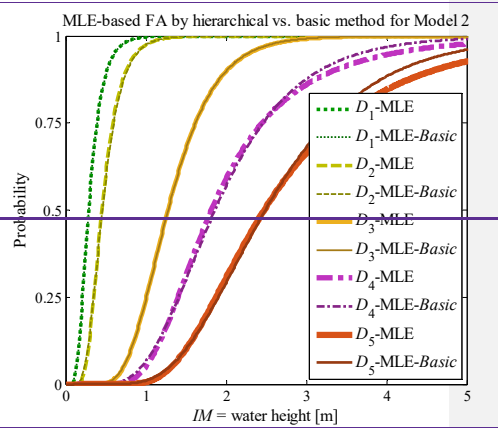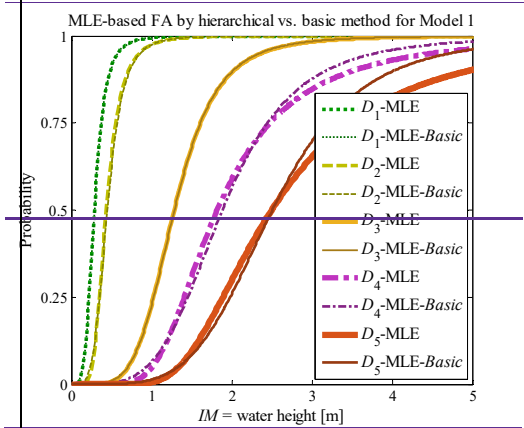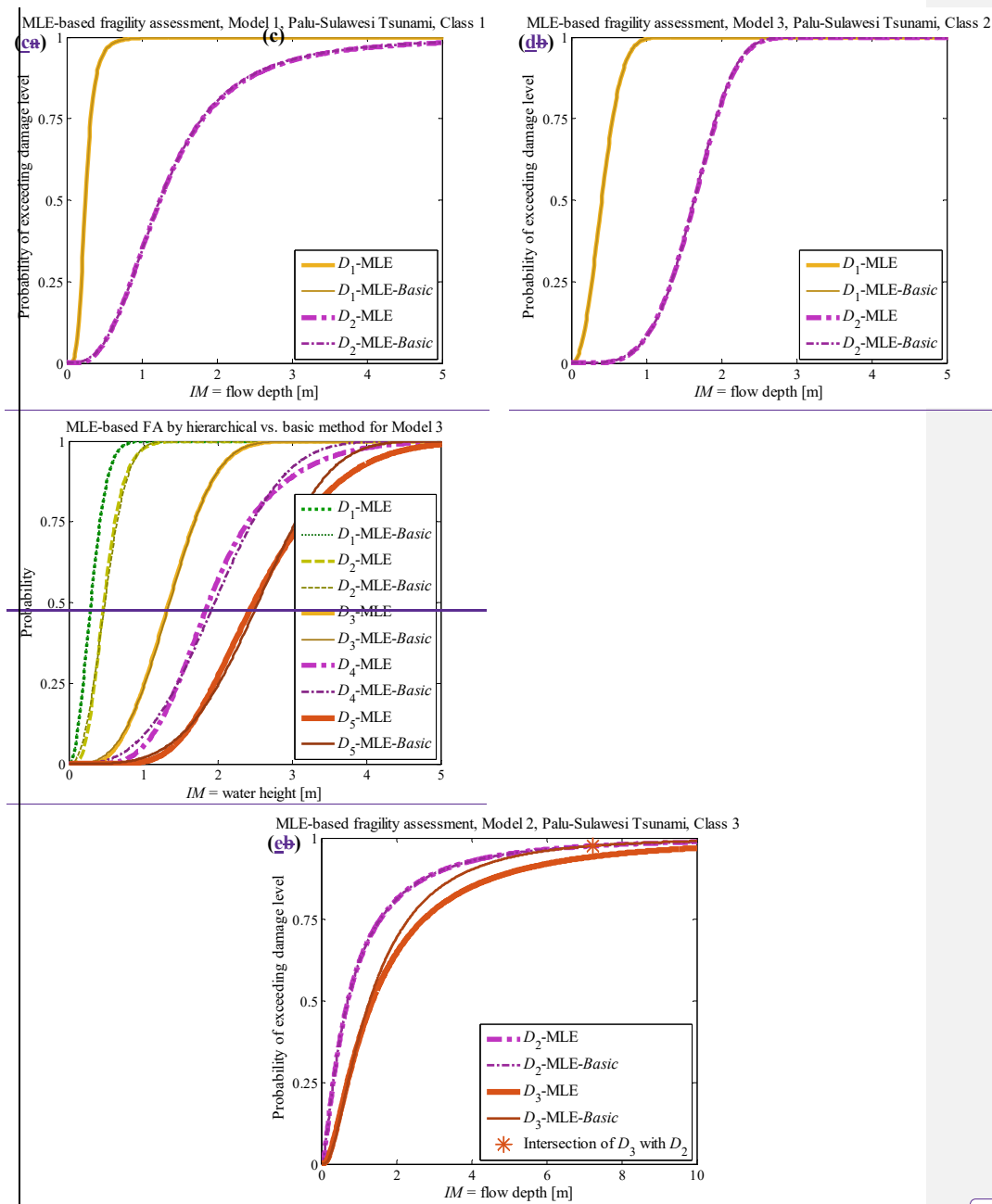
Figure 57: (a) Comparison between the fragility assessmentFA by MLE-based hierarchical fragility modeling and ~~direct FA based on~~ MLE-*Basic* fragility assessmentmethod given (a) South Pacific 2009 Tsunami , Class 1, $\mathbb{M}_{13}$; (b) South Pacific 2009 Tsunami, Class 2, $\mathbb{M}_{13}$; $)$ $\mathbb{M}_2$ and (c) Palu-Sulawesi 2018

640

To have a better comparison among the fragility curves in Figure 5, Table 6 reports the fragility assessmentFA parameters of the MLE and MLE-*Basic* methods for the damage thresholds $D_{index(2)}$ to $D_{index(N)5}$ with the equivalent lognormal parameters η_{IM_C} and β_{IM_C} (explained in Section 2.5) for $\mathbb{M}_1$ to $\mathbb{M}_3$ for all five classes considered. The medians are almost identical among the four models while there are higher dispersion estimates for MLE method derived by hierarchical fragility modelling. It is noteworthy that the fragility curves derived based on the MLE-*Basic* method do not intersect here; however, this condition was not explicitly enforced as it was in the hierarchical method.

Table 6: Comparison between fragility assessmentFA based on MLE method (by hierarchical fragility modelling) and the MLE-*Basic* method for damage thresholds $D_{1index(2)}$ to $D_{index(N)5}$.

Tsunami	Class	Damage Level	Model 1 ($\mathbb{M}_1$) MLE method η_{IM_C}[m]	β_{IM_C}	MLE-*Basic* method η_{IM_C}[m]	β_{IM_C}	Model 2 ($\mathbb{M}_2$) MLE method η_{IM_C}[m]	β_{IM_C}	MLE-*Basic* method η_{IM_C}[m]	β_{IM_C}	Model 3 ($\mathbb{M}_3$) MLE method η_{IM_C}[m]	β_{IM_C}	MLE-*Basic* method η_{IM_C}[m]	β_{IM_C}
South Pacific 2009	1	D_1	0.29	0.40	0.29	0.40	0.29	0.46	0.29	0.46	0.30	0.59	0.30	0.59
		D_2	0.43	0.35	0.45	0.37	0.45	0.38	0.46	0.40	0.47	0.44	0.48	0.50
		D_3	1.28	0.34	1.28	0.34	1.27	0.35	1.28	0.35	1.34	0.38	1.35	
		D_4	1.82	0.43	1.88	0.40	1.82	0.42	1.86	0.41	1.88	0.38	1.96	
		D_5	2.50	0.46	2.50	0.36	2.47	0.44	2.49	0.40	2.49	0.34	2.54	
	2	D_3	0.47	1.10	0.47	1.10	0.49	1.10	0.49	1.10	0.49	1.37	0.49	
		D_4	0.56	1.12	0.56	1.20	0.59	1.11	0.58	1.15	0.62	1.25	0.63	
		D_5	1.54	0.30	1.62	0.28	1.55	0.30	1.63	0.28	1.58	0.28	1.69	0.30
Sulawesi-Palu 2018	1	D_1	0.25	0.38	0.25	0.38	0.25	0.43	0.25	0.43	0.25	0.57	0.25	0.57
		D_2	1.24	0.57	1.24	0.57	1.24	0.58	1.24	0.58	1.30	0.57	1.30	
	2	D_1	0.38	0.45	0.38	0.45	0.38	0.47	0.38	0.47	0.40	0.53	0.40	0.53
		D_2	1.63	0.32	1.62	0.32	1.62	0.33	1.62	0.33	1.64	0.28	1.64	
	3	D_2	0.71	1.21	0.71	1.21	0.71	1.18	0.71	1.18	0.74	1.11	0.74	1.11
		D_3	1.38	1.10	1.31	0.91	1.36	1.02	1.29	0.88	1.32	0.84	1.31	0.76

Discussion: The results outlined in this section show fragility assessment for two different datasets corresponding to observed damaged in the aftermath of South Pacific and Sulawesi-Palu tsunami events. We have demonstrated the versatility of the proposed workflow and tool for hierarchical fragility assessment both for cases in which a large number of data points are available (e.g., Class 1, brick masonry residential, South Pacific Tsunami, Class 1, one-storey non-engineered masonry, Palu-Sulawesi Tsunami) and cases where very few data points are available (e.g., Class 2, timber residential, South Pacific Tsunami, Class 3, non-engineered light timber, Sulawesi-Palu Tsunami). Moreover, we demonstrated how the proposed workflow avoids crossing fragility curves (e.g., Class 2, timber residential, South Pacific Tsunami, Class 3, non-engineered light timber, Sulawesi-Palu Tsunami). The results illustrated for the five building classes demonstrate that the proposed workflow for hierarchical

fragility assessment can be applied in cases in which data points are not available for all the damage levels within the damage scale.

Conclusion

675 An integrated procedure based on Bayesian model class selection (BMCS) for empirical hierarchical fragility modeling for a class of buildings or infrastructure is presenteddiscussed. This procedure is applicable to fragility modelling for any type of hazard as long as This procedure relies on efficient simulation techniques to:the damage scale consists of mutually exclusive and collectively exhaustive (MECE) damage states and the observed damage data points are independent. This simulation-based
680 procedure can: –1) perform hierarchical fragility modeling for mutually exclusive and collectively exhaustiveMECE damage states; 2) estimate the confidence interval for the resulting fragility curves; 3) select the simplest model that fits the data best (i.e., maximizes log evidence) amongst a suite of candidate fragility models (herein, alternative link functions for generalized linear regression are considered). The proposed procedure is demonstrated for empirical fragility assessment based on
685 observed damage data to masonry residential (1 storey) and timber residential buildings due to the 2009 South Pacific Tsunami in the American Samoa and Samoa Islands and non-engineered masonry buildings (1 and 2 storeys) and non-engineered light timber buildings due to the 2018 Sulawesi-Palu Tsunami. It is observed that:

- For each model class, the same set of simulation realizations is used to estimate the fragility
690 parameters, the confidence band, and the log evidence. The latter, which consists of two terms depicting the goodness of fit and the information gain between posterior distribution resulting from the observed data and the prior distribution, is used to compare the candidate fragility models to identify the model that maximizes the evidence.
- Hierarchical fragility assessment can be done also based the maximum likelihood estimation
695 (MLE) and the available statistical toolboxes (e.g., MATLAB's generalized linear model). For each damage level, the reference domain should be the subset of data that exceeds the consecutive lower damage level, instead of taking the entire set of data points as reference domain. Note that the basic fragility estimation ("MLE-*Basic*", non-hierarchical fragility model)(MLE-*Basic*) fits the damage data for each damage level at a time. In other words, the reference domain is set to all
700 damage data.
- The procedure is applicable also to cases in which observed data is available only for a subset of the damage levels within the damage scale. The number of fragility curves is going to be equal to the total number of damage levels for which data is available minus one. This means, in order to have at least one fragility curve, one needs to have data available at least for two damage levels.
705 - Although the resulting fragility curves are not lognormal (strictly speaking), equivalent statistics work quite well inare used to showing the fragility curves (median and logarithmic dispersion) and the corresponding epistemic uncertainty (logarithmic dispersion).
- The results show that the fragility curves built based on "cloglog" link function lead to the highest evidence compared to the fragility curves obtained based on the other two link functions "logit"
710 and "probit".
- Moreover, tThe proposed method BMCS method and the one based on maximum likelihood estimation (MLE) lead to essentially the same set of parameters' estimates for hierarchical fragility estimation. However, the latter does not readily lead to the confidence band and log evidence.
-

Formattato: Rientro: Sinistro: 0 cm, Sporgente 0.75 cm

Formattato: Rientro: Sinistro: 0 cm, Sporgente 0.75 cm

Formattato: Rientro: Sinistro: 0 cm, Sporgente 0.75 cm

- Using the basic method for fragility estimation ("MLE-*Basic*", non-hierarchical fragility model) leads to results that are slightly different from the hierarchical fragility curves. The difference grows for higher damage levels. It is to note that following the basic method "MLE-*Basic*" did not lead to ill-conditioned results (i.e., fragility curves crossing) in some of the cases (Class 2 for South Pacific Tsunami, and Class 3 for Sulawesi-Palu Tsunami, both Timber constructions) studied in this work the case-study presented herein. Nevertheless, it is not guaranteed that, through following the basic method, the crossing fragility curves are going to be avoided.
-

The major improvement offered by this method is in providing a tool that can fit fragility curves to a set of hierarchical levels of damage or loss in an ensemble manner. This method, which starts from prescribed fragility models and explicitly ensures the hierarchical relation between the damage levels, is very robust to cases where few data points are available and/or where data is missing for some of the damage levels. This tool provides confidence bands for the fragility curves and performs model selection among a set of viable link functions for generalized regression. It is to note that the proposed method is in general applicable to hierarchical vulnerability modelling for human or economic loss levels and to different types of hazards, if (1) the defined levels are mutually exclusive and collectively exhaustive; and (2) a suitable intensity measure (IM) can be identified. The proposed method is quite general with respect for empirical fragility modelling and is transferable also to other types of hazards. This procedure is based on the assumption that given the intensity values, the set of observed damage data are independent.

Acknowledgements

The authors would like to acknowledge partial support from Horizon Europe Project Geo-INQUIRE. Geo-INQUIRE is funded by the European Commission under project number 101058518 within the HORIZON-INFRA-2021-SERV-01 call. The authors are grateful to the anonymous reviewer and Professor Carmine Galasso for their insightful and constructive comments.

Appendix A: The derivation of Equation (2)

The probability of being in damage state DS_j for a given intensity measure IM can be estimated as follows:

$$
\begin{aligned}
P\left(DS_j \middle| IM\right) &= P\left[\left(D \geq D_j\right) \cdot \left(D < D_{j+1}\right) \middle| IM\right] = 1 - P\left[\overline{\left(D \geq D_j\right) \cdot \left(D < D_{j+1}\right)} \middle| IM\right] \\
&= 1 - P\left[\overline{\left(D \geq D_j\right)} + \overline{\left(D < D_{j+1}\right)} \middle| IM\right] = 1 - \underbrace{P\left[\left(D < D_j\right) + \left(D \geq D_{j+1}\right) \middle| IM\right]}_{\text{ME} \therefore = P\left(D<D_j|IM\right)+P\left(D\geq D_{j+1}|IM\right)} \\
&= 1 - P\left(D < D_j \middle| IM\right) - P\left(D \geq D_{j+1} \middle| IM\right) = P\left(D \geq D_j \middle| IM\right) - P\left(D \geq D_{j+1} \middle| IM\right)
\end{aligned}
\tag{A1}
$$

745

where the upper-bar sign stands for the logical negation and is read as "NOT", and (+) defines the logical sum and is read as "OR". The above derivation is based on the *rule of sum* in probability and considering the fact that the two statements $D < D_j$ and $D \geq D_{j+1}$ are mutually exclusive (ME); thus, the probability of their logical sum is the sum of their probabilities.

750 **Appendix B: The derivation of Equation (7)**

The probability of being in damage state DS_j (where $j \geq 1$) given the intensity measure evaluated at the location of building i, denoted as IM_i, based on Equation (6) can be expanded in a recursive format as follows:

$$
\begin{aligned}
P\left(DS_j \middle| IM_i\right) &= \underbrace{\left[1 - P\left(D \geq D_{j+1} \middle| D \geq D_j, IM_i\right)\right]}_{1-\pi_{ij}} \cdot \left[1 - P\left(D < D_j \middle| IM_i\right)\right] \\
&= \left(1 - \pi_{ij}\right) \cdot \left[1 - P\left(\left(D < D_j\right) \cdot \left(D \geq D_{j-1}\right) + \cdots + \left(D < D_1\right) \cdot \left(D \geq D_0\right) \middle| IM_i\right)\right] \\
&= \left(1 - \pi_{ij}\right) \cdot \left[1 - \sum_{k=0}^{j-1} P\left(\left(D < D_{k+1}\right) \cdot \left(D \geq D_k\right) \middle| IM_i\right)\right] \\
&= \left(1 - \pi_{ij}\right) \cdot \left[1 - \sum_{k=0}^{j-1} P\left(DS_k \middle| IM\right)\right]
\end{aligned}
\tag{B1}
$$

755 where (+) defines the logical sum and is read as "OR". The above derivation is based on the rule of sum in probability and considering the fact that the recursive statements in the second term expressed generally as $(D < D_{k+1}) \cdot (D \geq D_k)$, where $0 \leq k \leq j - 1$, are ME; hence, the probability of their logical sum is the sum of their probabilities. It is to note that in case where $j=0$, the above equation can be written as:

760
$$
P\left(DS_0 \middle| IM_i\right) = \left(1 - \pi_{i0}\right) \triangleq P\left(D < D_1 \middle| IM_i\right)
\tag{B2}
$$

Appendix C: The derivation of log-evidence in Equation (13)

From an information-based point of view, the logarithm of the evidence (*log-evidence*), denoted as
765 $\ln[p(\mathbf{D}|\mathbb{M}_k)]$, can provide a quantitative measure of the amount of information as evidence of model $\mathbb{M}_k$. Moreover, the posterior PDF $p(\theta_k \theta | \mathbf{D}, \mathbb{M}_k)$ (see Equation 14) over the domain of the model parameters Ω_θ given the kth model is equal to unity. Thus, $\ln[p(\mathbf{D}|\mathbb{M}_k)]$ can be written as follows:

$$\ln\left[p\left(\mathbf{D}|\mathbb{M}_k\right)\right]=\ln\left[p\left(\mathbf{D}|\mathbb{M}_k\right)\right]\cdot\underbrace{\int_{\Omega\boldsymbol{\theta}_k}p\left(\boldsymbol{\theta}_k|\mathbf{D},\mathbb{M}_k\right)\mathrm{d}\boldsymbol{\theta}_k}_{=1.0} \tag{C1}$$

Since the log-evidence is independent of $\boldsymbol{\theta}$, we can bring it inside the integral, and do some simple manipulation (also using the relation in Equation 11) as follows:

$$\ln\left[p\left(\mathbf{D}|\mathbb{M}_k\right)\right]=\int_{\Omega\boldsymbol{\theta}_k}\ln\left[p\left(\mathbf{D}|\mathbb{M}_k\right)\right]\cdot p\left(\boldsymbol{\theta}_k|\mathbf{D},\mathbb{M}_k\right)\mathrm{d}\boldsymbol{\theta}_k$$

$$=\int_{\Omega_{\boldsymbol{\theta}}}\ln\left[\frac{p\left(\mathbf{D}|\boldsymbol{\theta}_k,\mathbb{M}_k\right)p\left(\boldsymbol{\theta}_k|\mathbb{M}_k\right)}{p\left(\boldsymbol{\theta}_k|\mathbf{D},\mathbb{M}_k\right)}\right]\cdot p\left(\boldsymbol{\theta}_k|\mathbf{D},\mathbb{M}_k\right)\mathrm{d}\boldsymbol{\theta}_k$$

$$=\int_{\Omega_{\boldsymbol{\theta}}}\ln\left[\frac{p\left(\mathbf{D}|\boldsymbol{\theta}_k,\mathbb{M}_k\right)}{p\left(\boldsymbol{\theta}_k|\mathbf{D},\mathbb{M}_k\right)\big/p\left(\boldsymbol{\theta}_k|\mathbb{M}_k\right)}\right]\cdot p\left(\boldsymbol{\theta}_k|\mathbf{D},\mathbb{M}_k\right)\mathrm{d}\boldsymbol{\theta}_k$$

$$=\underbrace{\int_{\Omega_{\boldsymbol{\theta}}}\ln\left[p\left(\mathbf{D}|\boldsymbol{\theta}_k,\mathbb{M}_k\right)\right]\cdot p\left(\boldsymbol{\theta}_k|\mathbf{D},\mathbb{M}_k\right)\mathrm{d}\boldsymbol{\theta}_k}_{Term\,1}-\underbrace{\int_{\Omega_{\boldsymbol{\theta}}}\ln\left[\frac{p\left(\boldsymbol{\theta}_k|\mathbf{D},\mathbb{M}_k\right)}{p\left(\boldsymbol{\theta}_k|\mathbb{M}_k\right)}\right]\cdot p\left(\boldsymbol{\theta}_k\mathbf{D},\mathbb{M}_k\right)\mathrm{d}\boldsymbol{\theta}_k}_{Term\,2} \tag{C2}$$

Appendix D: Multivariate normal distribution and generating dependent Gaussian variables

Let us assume that the vector of parameters for the kth model is set to $\boldsymbol{\theta}$; i.e., $\boldsymbol{\theta}=\boldsymbol{\theta}_k$. A multivariate normal PDF can be expressed as follows:

$$p\left(\boldsymbol{\theta}\right)=\frac{1}{\sqrt{\left(2\pi\right)^n|\mathbf{S}|}}\exp\left(-\frac{1}{2}\left(\boldsymbol{\theta}-\boldsymbol{\mu_\theta}\right)^{\mathrm{T}}\mathbf{S}^{-1}\left(\boldsymbol{\theta}-\boldsymbol{\mu_\theta}\right)\right) \tag{D1}$$

where n is the number of components (uncertain parameters) of vector $\boldsymbol{\theta}=\{\theta_i, i=1:n\}$; $\boldsymbol{\mu_\theta}$ is the vector of the mean value of $\boldsymbol{\theta}$; $\mathbf{S}$ is the covariance matrix. The positive definite matrix $\mathbf{S}_{n\times n}$ can be factorized based on Cholesky decomposition as $\mathbf{S}=\mathbf{L}\mathbf{L}^T$, where $\mathbf{L}_{n\times n}$ is a lower triangular matrix (i.e., for all $j>i$, $L_{ij}=0$ where L_{ij} denotes the (i,j)-entry of the matrix $\mathbf{L}$). A Gaussian vector $\boldsymbol{\theta}_{n\times1}$ with mean $\boldsymbol{\mu_\theta}$ and covariance $\mathbf{S}$ can be generated as follows:

$$\boldsymbol{\theta}=\boldsymbol{\mu_\theta}+\mathbf{L}\mathbf{Z} \tag{D2}$$

where $\mathbf{Z}_{n\times1}$ is a vector of standard Gaussian $i.i.d.$ random variables with zero mean $\mathbf{0}_{n\times n}$, and covariance equal to the identity matrix $\mathbf{I}_{n\times n}$. To verify the properties of $\boldsymbol{\theta}$, we know that with reference to Equation (D2), it should have a mean equal to $\boldsymbol{\mu_\theta}$ and a covariance matrix equal to $\mathbf{S}$. The expectation of $\boldsymbol{\theta}$, denoted as $\mathrm{E}(\boldsymbol{\theta})$, can be estimated as:

$$\mathrm{E}\left(\boldsymbol{\theta}\right)=\mathrm{E}\left(\boldsymbol{\mu_\theta}+\mathbf{L}\mathbf{Z}\right)=\mathrm{E}\left(\boldsymbol{\mu_\theta}\right)+\mathbf{L}\underbrace{\mathrm{E}\left(\mathbf{Z}\right)}_{=\mathbf{0}_{n\times1}}=\boldsymbol{\mu_\theta} \tag{D3}$$

The covariance matrix of $\boldsymbol{\theta}$ can be written as:

$$\mathrm{E}\left[\left(\boldsymbol{\theta}-\boldsymbol{\mu_\theta}\right)\left(\boldsymbol{\theta}-\boldsymbol{\mu_\theta}\right)^T\right]=\mathrm{E}\left(\mathbf{L}\mathbf{Z}\mathbf{Z}^T\mathbf{L}^T\right)=\mathbf{L}\underbrace{\mathrm{E}\left(\mathbf{Z}\mathbf{Z}^T\right)}_{=\mathbf{I}_{n\times n}}\mathbf{L}^T=\mathbf{L}\mathbf{L}^T=\mathbf{S} \tag{D4}$$

Thus, the vector $\boldsymbol{\theta}$ can be written according to Equation (D2).

Appendix E: Adaptive MCMC scheme

MCMC procedure

The MCMC simulation scheme has a Markovian nature where the transition from current state to a new
795 state is done by using a conditional transition function that is conditioned on the current (last) state. Let us assume that the vector of parameters for the *k*th model is set to $\boldsymbol{\theta}$; i.e., $\boldsymbol{\theta} = \boldsymbol{\theta}_k$. To generate $(i+1)^{\text{th}}$ sample $\boldsymbol{\theta}_{i+1}$ from the current i^{th} sample $\boldsymbol{\theta}_i$ based on MH routine, the following procedure is adopted herein:
- Simulate a *candidate* sample $\boldsymbol{\theta}^*$ from a *proposal* distribution $q(\boldsymbol{\theta}|\boldsymbol{\theta}_i)$. It is important to note that
800 there are no specific restrictions about the choice of $q(\cdot)$ apart from the fact that it should be possible to calculate both $q(\boldsymbol{\theta}_{i+1}|\boldsymbol{\theta}_i)$ and $q(\boldsymbol{\theta}_i|\boldsymbol{\theta}_{i+1})$.
- Calculate the acceptance probability $\min(1,r)$, where r is defined as follows (it is to note that the following Equation (E1) is written in the general format for brevity compared to Equation (14) of the manuscript, and we have used $\boldsymbol{\theta}$ instead of $\boldsymbol{\theta}_k$, and dropped the conditioning on $\mathbb{M}_k$; hence when
805 we write the ith sample $\boldsymbol{\theta}_i$, it is actually the ith sample drawn from $\boldsymbol{\theta}_k$ and "k" is dropped for brevity):

$$
r = \frac{p(\boldsymbol{\theta}^*|\mathbf{D})}{p(\boldsymbol{\theta}_i|\mathbf{D})} \cdot \frac{q(\boldsymbol{\theta}_i|\boldsymbol{\theta}^*)}{q(\boldsymbol{\theta}^*|\boldsymbol{\theta}_i)} = \left(\underbrace{\frac{p(\mathbf{D}|\boldsymbol{\theta}^*)}{p(\mathbf{D}|\boldsymbol{\theta}_i)}}_{\text{likelihood ratio}} \cdot \underbrace{\frac{p(\boldsymbol{\theta}^*)}{p(\boldsymbol{\theta}_i)}}_{\text{prior ratio}} \right) \cdot \underbrace{\frac{q(\boldsymbol{\theta}_i|\boldsymbol{\theta}^*)}{q(\boldsymbol{\theta}^*|\boldsymbol{\theta}_i)}}_{\text{proposal ratio}}
\tag{E1}
$$

- Generate u from a Uniform distribution between (0, 1), $u \sim$ Uniform (0, 1).
- if $u \leq \min(1,r) \rightarrow$ set $\boldsymbol{\theta}_{i+1}=\boldsymbol{\theta}^*$ (*accept* the *candidate* state to be taken as the *next* state of the Markov chain); else set $\boldsymbol{\theta}_{i+1}=\boldsymbol{\theta}_i$ (the *current* state is taken as the *next* state).

810 Estimating the likelihood in the arithmetic scale based on Equation (E1) may encounter instability as $p(\mathbf{D}|\boldsymbol{\theta})$ may become very small; thus, the likelihood ratio becomes indeterminate. To avoid this numerical instability, it is desirable to substitute the likelihood ratio in Equation (E1) with $\exp(\ln(p(\mathbf{D}|\boldsymbol{\theta}^*)) - \ln(p(\mathbf{D}|\boldsymbol{\theta}_i)))$ if the ratio becomes indeterminate or zero.

With reference to Equation (E1), samples from the posterior can be drawn based on MH algorithm
815 without any need to define the normalizing C^{-1} coefficient according to Equation (14). Equation (E1) always accepts a candidate if the new proposal is more likely under the target posterior distribution than the old state. Therefore, the sampler will move towards the regions of the state space where the target posterior function has high density.

The choice of the proposal distribution q is very important. The ratio $q(\boldsymbol{\theta}_i|\boldsymbol{\theta}^*)/q(\boldsymbol{\theta}^*|\boldsymbol{\theta}_i)$ corrects for any
820 asymmetries in the proposal distribution. Intuitively, if $q(\boldsymbol{\theta}^*|\boldsymbol{\theta}_i)=p(\boldsymbol{\theta}^*|\mathbf{D})$, the candidate state is always accepted (with r=1); thus the closer q is to the target posterior PDF, the better the acceptance rate and the faster the convergence. This is not a trivial task as information about the important region $p(\boldsymbol{\theta}|\mathbf{D})$ is not available. If the proposal distribution q is *non-adaptive*, it means that the information of the current sample $\boldsymbol{\theta}_i$ is not used to explore the important region of the target posterior distribution $p(\boldsymbol{\theta}|\mathbf{D})$; thus, we
825 can say that $q(\boldsymbol{\theta}^*|\boldsymbol{\theta}_i)= q(\boldsymbol{\theta}^*)$. Therefore, it is more desirable to choose an *adaptive* proposal distribution which depends on the current sample (Beck and Au 2002). Having the proposal PDF q centered around the current sample renders the MH algorithm like a local random walk that adaptively leads to the generation of the target PDF. However, if the Markov chain starts from a point that is not close to region

of the significant probability density of $p(\mathbf{\theta}|\mathbf{D})$, the chance of generating a candidate state $\mathbf{\theta}^*$ will become
830 extremely small (and we will face high rejection of candidate samples). Therefore, most of the samples
will be repeated. To solve this problem, Beck and Au (2002) introduce a sequence of PDFs that bridge
the gap between the prior PDF and the target posterior PDF. This issue will be more explored hereafter
under the adaptive MCMC. Finally, it can mathematically be shown that (see Beck and Au 2002) if the
current sample $\mathbf{\theta}_i$ is distributed as $p(\cdot|\mathbf{D})$, the next sample $\mathbf{\theta}_{i+1}$ is also distributed as $p(\cdot|\mathbf{D})$.

835 ***Adaptive Metropolis-Hastings algorithm (adaptive MCMC)***

The adaptive MH algorithm (Beck and Au 2002) introduces a sequence of intermediate candidate
evolutionary PDF's that resemble more and more the target PDF. Let $\{p_1, p_2,\ldots, p_{Nchain}\}$ be the sequence
(*chain*) of PDF's leading to $p(\mathbf{\theta}|\mathbf{D})=p_{Nchain}$, where *Nchain* is the number of chains and each chain
contains N_{seed} samples (as indicated subsequently). The following adaptive simulation-based procedure
840 is employed:

Step 1: Simulate $\underline{N_d}$ ~~Nseed~~ samples $\{\mathbf{\theta}_1, \mathbf{\theta}_2, \ldots, \mathbf{\theta}_{Nseed}\}^{(1)}$, where the superscript (1) denotes the first
simulation level or the first chain (nc=1 where nc denotes the chain number/simulation level), with the
target PDF p_1 as the first sequence of samples. Instead of accepting or rejecting a proposal for $\mathbf{\theta}$
involving all its components simultaneously (called *block-wise* updating scheme), it might be
845 computationally simpler and more efficient for the first chain to make proposals for individual
components of $\mathbf{\theta}$, one at a time (called *component-wise* updating approach). In the *block-wise* updating,
the proposal distribution has the same dimension as the target distribution. For instance, if the model
parameters involve n uncertain parameters (e.g., the vector of model parameters $\mathbf{\theta}_{n\times1}$ in this paper has
$n = 2$~~(N_{DS} − 1) = 8~~N variables for each of the three models $\mathbb{M}_1$, $\mathbb{M}_2$, and $\mathbb{M}_3$), we design an n-
850 dimensional proposal distribution, and either accept or reject the candidate state (with all n variables)
as a block. The block-wise updating approach can be associated with high rejection rates. This may
cause problem when we want to generate the first sequence of samples (first chain). Therefore, we have
utilized the more stable component-wise updating for the first chain. We start from the first variable
and generate a candidate state based on a proposal distribution for this individual component, and finally
855 accept or reject it based on MH algorithm. Note that in this stage, we have varied the current component
and kept the other variables in vector $\mathbf{\theta}$ constant. Then, we move to the next components one by one
and do the same procedure while taking into account the previous (updated) components. Therefore,
what happens in the current step is conditional on the updated parameters in the previous steps.

Step 2: Construct a kernel density function $\kappa^{(1)}$ as the weighted sum (average) of n-dimensional
860 Gaussian PDFs centered among the samples $\{\mathbf{\theta}_1, \mathbf{\theta}_2, \ldots, \mathbf{\theta}_{Nseed}\}^{(1)}$, with the covariance matrix $\mathbf{S}^{(1)}$ of the
samples $\mathbf{\theta}_i^{(1)}$ and the weights associated to each sample as w_i where i=1: $\underline{N_d}$ ~~Nseed~~ as follows (see Ang
et al. 1992, Au and Beck 2002):

$$\kappa^{(1)}(\mathbf{\theta}) = \frac{1}{Nseed} \sum_{i=1}^{Nseed} \frac{1}{w_i^n \sqrt{(2\pi)^n |\mathbf{S}^{(1)}|}} \exp\left(-\frac{1}{2w_i^2}\left(\mathbf{\theta}-\mathbf{\theta}_i^{(1)}\right)^{\mathrm{T}}\left(\mathbf{S}^{(1)}\right)^{-1}\left(\mathbf{\theta}-\mathbf{\theta}_i^{(1)}\right)\right) \qquad (E2)$$

The kernel density $\kappa^{(1)}$ constructed in Equation (E2) approximates p_1. The kernel function κ can be
865 viewed as a PDF consisting of bumps at $\mathbf{\theta}_i$, where width w_i controls the common size of the bumps.
Therefore, a large value of w_i tends to over-smooth the kernel density, while a small value may cause
noise-shaped bumps. In view of this, w_i can be assumed to have a fixed width ($= w$), or alternatively the
adaptive kernel estimate can be employed (Ang et al. 1992, Au and Beck 1999) that is defined for each
sample $\mathbf{\theta}_i$, i=1: $\underline{N_d}$ ~~Nseed~~. The adaptive kernel has better convergence and smoothing properties over
870 the fixed-width kernel estimate. The fixed width w is estimated as follows (Epanechnikov 1969):

$$w = \left(\frac{4}{(n+2)N_{dist}} \right)^{\frac{1}{n+4}} \tag{E3}$$

where N_{dist} is the number of distinct samples ($N_{dist} \leq N_d \overline{Nseed}$). For one-dimensional problems ($n=1$), this leads to the well-known fixed-width value of $[(4/3)/Nseed]^{1/5}$. The reason for using N_{dist} is due to the fact that for the next simulation levels, where we are going to use a block-wise updating approach in the MCMC scheme, one may be faced with rejection of candidate states within the Markov chain. Thus, we need to count the distinct samples. In the adaptive kernel method, the idea is to vary the shape of each bump so that a larger width (flatter bump) is used in regions of lower probability density. Following the general strategy used in the past (see Ang et al. 1992, Au and Beck 1999), the adaptive band width w_i for the ith sample $\boldsymbol{\theta}_i$ can be written as $w_i = w\lambda_i$, where the local bandwidth factor λ_i can be estimated as follows:

$$\lambda_i = \left(\kappa(\boldsymbol{\theta}_i) \middle/ \left(\prod_{j=1}^{Nseed} \kappa(\boldsymbol{\theta}_j) \right)^{\frac{1}{Nseed}} \right)^{-\omega} \tag{E4}$$

where $0 \leq \omega \leq 1.0$ is the sensitivity factor, and $\kappa(\boldsymbol{\theta}_i)$ is calculated based on Equation (E2) where $\boldsymbol{\theta}=\boldsymbol{\theta}_i$, with the choice of fixed-width w in Equation (E3). The denominator in Equation (E4) is a geometric mean of the kernel estimator at all $N_d \overline{Nseed}$ points. The value of $\omega = 0.50$ is employed herein as also suggested by other research endeavors (Abramson 1982, Ang et al. 1992, Au and Beck 1999). It is numerically more stable to estimate the denominator in Equation (E4) as $\prod_{j=1}^{Nseed} \left[\kappa(\boldsymbol{\theta}_j)^{1/Nseed} \right]$.

Step 3: Simulate $N\overline{seed}$ Markov chain samples $\{\boldsymbol{\theta}_1, \boldsymbol{\theta}_2, ..., \boldsymbol{\theta}_{Nseed}\}^{(2)}$ with the target PDF p_2 as the second simulation level ($nc=2$). We use $\kappa^{(1)}$ as the proposal distribution $q(\cdot)$ in Equation (E1) in this stage to generate the second chain of samples. To generally simulate sample $\boldsymbol{\theta}$ from the kernel $\kappa^{(nc)}$ (where $nc=1$:$Nchain$), we generate a discrete random index from the vector $[1, 2, ..., N_d \overline{Nseed}]$ with the corresponding weights $[w_1, w_2, \cdots, w_{Nseed}]$ using an inverse transformation sampling; if index=j, then generate $\boldsymbol{\theta}$ from the Gaussian PDF κ_j, where:

$$\begin{aligned}
\kappa_j(\boldsymbol{\theta}) &= \frac{1}{\left(w\lambda_j\right)^n \sqrt{(2\pi)^n |\mathbf{S}^{(nc)}|}} \cdot \exp\left(-\frac{1}{2\left(w\lambda_j\right)^2} \left(\boldsymbol{\theta}-\boldsymbol{\theta}_j\right)^{\text{T}} \left(\mathbf{S}^{(nc)}\right)^{-1} \left(\boldsymbol{\theta}-\boldsymbol{\theta}_j\right) \right) \\
&= \frac{1}{\sqrt{(2\pi)^n |\mathbf{S}_j^{(nc)}|}} \cdot \exp\left(-\frac{1}{2} \left(\boldsymbol{\theta}-\boldsymbol{\theta}_j\right)^{\text{T}} \left(\mathbf{S}_j^{(nc)}\right)^{-1} \left(\boldsymbol{\theta}-\boldsymbol{\theta}_j\right) \right)
\end{aligned} \tag{E5}$$

where $\mathbf{S}_j^{(nc)} = w_j{}^2 \mathbf{S}^{(nc)}$, where $\mathbf{S}^{(nc)}$ is the covariance matrix of the samples $\{\boldsymbol{\theta}_1, \boldsymbol{\theta}_2, ..., \boldsymbol{\theta}_{Nseed}\}^{(nc)}$. Appendix D shows how a sample $\boldsymbol{\theta}$ can be drawn from the Gaussian PDF κ_i. From this sequence on, the MCMC updating is done in a block-wise manner as we generate a candidate $\boldsymbol{\theta}$ and accept/reject it as a block. The second chain of samples $\{\boldsymbol{\theta}_1, \boldsymbol{\theta}_2, ..., \boldsymbol{\theta}_{Nseed}\}^{(2)}$ are then used to construct the kernel density $\kappa^{(2)}$ based on Equation (E2).

Step 4: In general, $\kappa^{(nc)}$ is used as the proposal distribution in order to move from the nc^{th} simulation level (which approximates p_{nc}) into $(nc+1)^{\text{th}}$ chain (with target PDF p_{nc+1}). This will continue until the $Nchain^{\text{th}}$ simulation level where Markov chain samples are simulated for the target updated $p(\boldsymbol{\theta}|\mathbf{D})=p_{Nchain}$.

Appendix F: MCMC samples for each model

The adaptive MCMC procedure for drawing samples from the model parameters from the joint posterior
905 PDF $p(\boldsymbol{\theta}_k|\mathbf{D}, \mathbb{M}_k)$ is carried out by considering *Nchain*=~~5~~ 6 chains (simulation levels), and
N_d~~*Nseed*=1000~~ 2000 samples per each chain (see Appendix E). In the first simulation level (first chain,
nc=1), for which a component-wise updating approach is employed (see Appendix E, **Step 1** for the
description of component-wise and block-wise updating), the first 20 samples are not considered in
order to reduce the initial transient effect of the Markov chain. The proposal distribution (see Equation
910 E1) for each component is assumed to be a normal distribution with a coefficient of variation
COV~~=1.6~~0.30 herein. In addition, the prior ratio according to Equation (E1), will become the ratio
of two normal distributions, for each component one at a time. In the next simulation levels (i.e., *nc*=2
~~to~~ :56), the adaptive kernel estimate (Equation E2) is employed, i.e., the MCMC updating is performed
in a block-wise manner. ~~Since tThis updating approach can be associated with high rejection rates (i.e.,~~
915 ~~there are similar samples indicating the rejection of the candidate states within the Markov chain),~~ there
will be ~~N_d~~ N_d ~~distinct (not considering the repeats)~~ Markov chain samples generated within the each
chain, denoted as $\{\boldsymbol{\theta}_{k,1}, \boldsymbol{\theta}_{k,2}, \cdots, \boldsymbol{\theta}_{k,N_d}\}^{(nc)}$, where ~~$N_d \leq$ *Nseed* and~~ *nc*=2:*Nchain* (=~~5~~6). The N_d
samples of the last chain (*nc*=6~~5~~) will be used as the fragility model parameters, as discussed in Section
3.4~~6~~. It is to note that the likelihood $p(\mathbf{D}|\boldsymbol{\theta}_k, \mathbb{M}_k)$ (used in calculating the acceptance probability within
920 the MCMC procedure in Equation E1) is estimated according to Equation (13).
Figure ~~2~~F1 illustrates the histograms representing the drawn samples from the joint posterior PDF's
corresponding to the sampled model parameters $\{\boldsymbol{\theta}_{k,1}, \boldsymbol{\theta}_{k,2}, \cdots, \boldsymbol{\theta}_{k,N_d}\}^{(56)}$ corresponding to the brick
masonry residential, Class~~es~~ 1~~-2~~ South Pacific Tsunami ~~and Classes 1-3 Sulawesi Palu, for the model~~
classes $\mathbb{M}_k$ ($k \in \{1,2,3\}$) shown in Figure 2 ~~to Figure 6~~. ~~related to $\mathbb{M}_k$ (where $k = 1:3$). For model $\mathbb{M}_1$,~~
925 ~~N_d=903< *Nseed*=1000; for model $\mathbb{M}_2$, N_d=882; finally, for $\mathbb{M}_3$, we have N_d=951.~~ The marginal normal
prior PDFs are also shown with orange-coloured dashed lines. The statistics of the samples ~~(,~~ mean and
~~COV~~ confidence interval (CI) between 2nd and 98th percentiles ~~of~~ for the posterior~~)~~ of model parameters
$\boldsymbol{\theta}_k$ are shown on the figures associated to each parameter. It is expected to have the mean values of the
marginal posterior samples close to and comparable with those obtained by the MLE in Table ~~2~~4~~(first~~
930 ~~row) that are also the mean values of prior joint PDF~~.
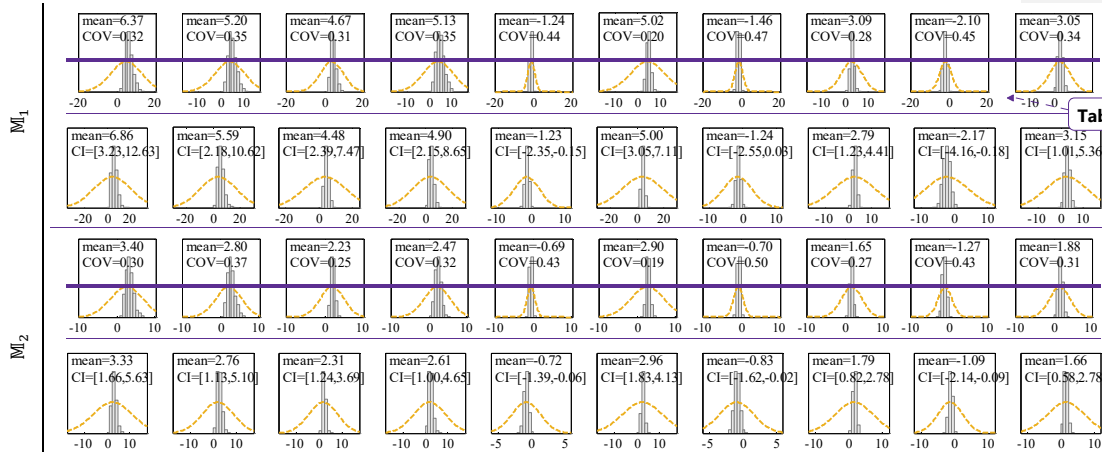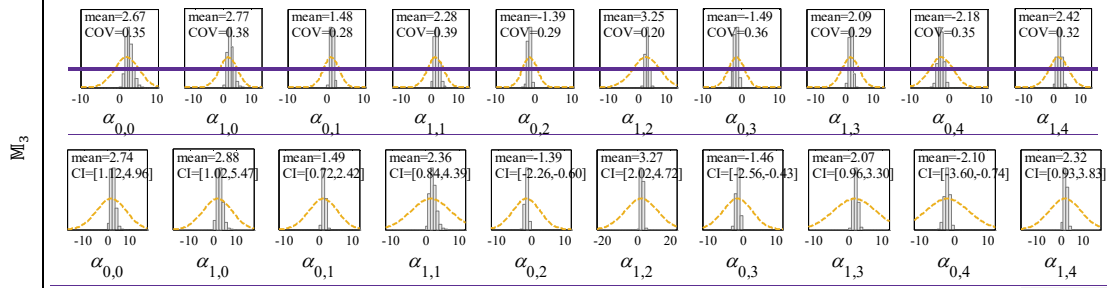
Figure F1: Distribution of the fragility model parameters $\theta_k = \left[\{\alpha_{0j}, \alpha_{1j}\}_k, j = 0:4\right]$ based on model class $\mathbb{M}_k$ (where $k = 1:3$) for Class 1, Brick masonry residential, South Pacific Tsunami, by employing an adaptive MCMC procedure including samples drawn from the joint posterior PDF with their statistics (mean and COV), and the marginal normal priors (subfigures show the posterior statistics).

935

Code availability

The code implementing the methodology in this article is available at the following URL:
https://github.com/eurotsunamirisk/computeFrag/tree/main/Code_ver2

940 ~~https://github.com/eurotsunamirisk/computeFrag~~

Data availability

The data used to produce the results in this article are available at the following URL:
https://github.com/eurotsunamirisk/computeFrag/tree/main/Code_ver2

~~https://github.com/eurotsunamirisk/computeFrag~~

945 **Author contribution**

FJ designed and coordinated this research. HE performed the simulations and developed the fragility functions. KT cured the availability of codes and software on the European Tsunami Risk Service (ETRiS). BB provided precious insights on the damage data gathered for American Samoa and Samoa Islands in the aftermath of the 2009 South Pacific Tsunami (documented in Reese et al 2011). All
950 authors have contributed to the drafting of the manuscript. The first two authors contributed in an equal manner to the drafting of the manuscript.

Competing interests:

The authors declare that they have no conflict of interest.

References

955 Abramson, I. S.: On bandwidth variation in kernel estimates–a square root law, *Ann. Stat.*, 10(4), 1217-1223, 1982.

Agresti, A.: *Categorical Data Analysis*, 3rd ed., Wiley, New York, 2012.

Ang, G. L., Ang, A. H.-S., and Tang, W. H.: Optimal importance sampling density estimator, *J. Eng. Mech.*, 118(6), 1146–1163, 1992.

960 Au, S. K., and Beck, J. L.: A new adaptive importance sampling scheme, *Struct. Saf.*, 21, 135–158, 1999.

Beck, J. L., and Yuen K.-V.: Model selection using response measurements: Bayesian probabilistic approach, *J. Eng. Mech.*, 130,192–203, 2004.

Behrens, J., Løvholt, F., Jalayer, F., Lorito, S., Salgado-Gálvez, M. A., Sørensen, M., ..., and
965 Vyhmeister, E.: Probabilistic Tsunami Hazard and Risk Analysis: A Review of Research Gaps, *Front. Earth Sci.*, 9, 114, 2021.

Cover, T. M., Thomas J. A.: *Elements of information theory*, Wiley, New York, 1991.

Charvet, I., Ioannou, I., Rossetto, T., Suppasri, A., and Imamura, F.: Empirical fragility assessment of buildings affected by the 2011 Great East Japan tsunami using improved statistical models, *Nat.*
970 *Hazards*, 73, 951–973, 2014.

Charvet, I., Suppasri, A., Kimura, H., Sugawara, D., and Imamura, F.: A multivariate generalized linear tsunami fragility model for Kesennuma City based on maximum flow depths, velocities and debris impact, with evaluation of predictive accuracy, *Nat Hazards*, 79(3), 2073-2099, 2015.

Charvet, I., Macabuag, J., and Rossetto, T.: Estimating tsunami-induced building damage through fragility functions: critical review and research needs, *Front. Built Environment*, 3, 36, 2017.

Chua, C. T., Switzer, A. D., Suppasri, A., Li, L., Pakoksung, K., Lallemant, D., ..., and Winspear, N.: Tsunami damage to ports: Cataloguing damage to create fragility functions from the 2011 Tohoku event, *Nat Hazards Earth Sys*, 21(6), 1887-1908, 2021.

De Risi, R., Goda, K., Mori, N., and Yasuda T.: Bayesian tsunami fragility modelling considering input data uncertainty, *Stoch. Env. Res. Risk A.*, 31, 1253–1269, 2017a.

De Risi, R., Goda, K., Yasuda, T., and Mori, N.: Is flow velocity important in tsunami empirical fragility modeling?, *Earth-Sci. Rev.*, 166, 64-82, 2017b.

Ebrahimian, H., and Jalayer, F: Selection of seismic intensity measures for prescribed limit states using alternative nonlinear dynamic analysis methods, *Earthq. Eng. Struct. D.*, 50(5), 1235-1250, 2021.

Eidsvig, U. M. K., Papathoma-Köhle, M., Du, J., Glade, T., and Vangelsten, B. V.: Quantification of model uncertainty in debris flow vulnerability assessment, *Eng. Geol.*, 181, 15-26, 2014.

Epanechnikov, V.A.: Nonparametric estimation of a multidimensional probability density. *Theor. Probab. Appl.*, 14, 153-1588, 1969.

Goff, J., and Dominey-Howes, D.: The 2009 South Pacific Tsunami, *Earth-Sci. Rev.*, 107(1–2), v-vii, 2011.

Grünthal, G. (1998), *European macroseismic scale 1998*, European Seismological Commission (ESC).

Hastings, W. K.: Monte-Carlo sampling methods using Markov chains and their applications, *Biometrika*, 57(1), 97-109, 1970.

Jalayer, F., Beck, J., and Zareian, F.: Analyzing the sufficiency of alternative scalar and vector intensity measures of ground shaking based on information theory, *J Eng Mech*, 138(3), 307-316, 2012.

Jalayer, F., De Risi, R., and Manfredi, G. Bayesian Cloud Analysis: efficient structural fragility assessment using linear regression, *B. Earthq. Eng.*, 13(4), 1183-1203, 2015.

Jalayer, F., Ebrahimian, H., Miano, A., Manfredi, G., and Sezen, H.: Analytical fragility assessment using unscaled ground motion records, *Earthq. Eng. Struct. D.*, 46(15), 2639-2663, 2017.

Jalayer, F., and Ebrahimian H.: Seismic reliability assessment and the non-ergodicity in the modelling parameter uncertainties, *Earthq. Eng. Struct. D.*, 49(5),434-457, 2020.

Jalayer, F., Ebrahimian, H., and Miano, A.: Intensity-based demand and capacity factor design: a visual format for safety-checking, *Earthq. Spectra*, 36(4):1952-1975. 2020

Koshimura, S., Namegaya, Y., and Yanagisawa, H.: Tsunami Fragility—A New Measure to Identify Tsunami Damage, *J. Disaster Research*, 4(6), 479-488, 2009a

Koshimura, S., Oie, T., Yanagisawa, H., and Imamura, F. (2009b). Developing fragility functions for tsunami damage estimation using numerical model and post-tsunami data from Banda Aceh, Indonesia, *Coas. Eng. J.*, 51(3), 243-273, 2009b.

Kullback, S., Leibler, R.A. (1951). On information and sufficiency. *Ann. Math. Stat.* 22(1), 79-86.

Lahcene, E., Ioannou, I., Suppasri, A., Pakoksung, K., Paulik, R., Syamsidik, S., ..., and Imamura, F.: Characteristics of building fragility curves for seismic and non-seismic tsunamis: case studies of the 2018 Sunda Strait, 2018 Sulawesi–Palu, and 2004 Indian Ocean tsunamis, *Nat. Hazards Earth Sys.*, 21(8), 2313-2344, 2021.

1015   Mas, E., Paulik, R., Pakoksung, K. et al. (2020). Characteristics of tsunami fragility functions developed using different sources of damage data from the 2018 Sulawesi earthquake and tsunami. *Pure Appl. Geophys.*, 177, 2437-2455.

Miano, A., Jalayer, F., Forte, G., and Santo, A.: Empirical fragility assessment using conditional GMPE-based ground shaking fields: Application to damage data for 2016 Amatrice Earthquake, *B.* 1020   *Earthq. Eng.*, 18(15), 6629-6659, 2020.

Metropolis, N., Rosenbluth, A. W., Rosenbluth, M. N., Teller, A. H., and Teller E.: Equations of state calculations by fast computing machines, *J. Chem. Phys.* 21(6), 1087-1092, 1953.

Muhari, A., Imamura, F., Arikawa, T., Hakim, A. R., & Afriyanto, B. (2018). Solving the puzzle of the September 2018 Palu, Indonesia, tsunami mystery: clues from the tsunami waveform and the initial 1025   field survey data. *J. Disaster Res.*, 13(Scientific Communication), sc20181108.

Muto, M., and Beck, J. L.: Bayesian updating and model class selection for hysteretic structural models using stochastic simulation, *J. Vib. Control*, 14(1-2),7-34, 2008.

Paulik, R., Gusman, A., Williams, J. H. et al. (2019). Tsunami hazard and built environment damage observations from Palu city after the September 28 2018 Sulawesi earthquake and tsunami. *Pure Appl.* 1030   *Geophys.* 176, 3305-3321.

Rafliana, I., Jalayer, F., Cerase, A., et al. (2022). Tsunami risk communication and management: Contemporary gaps and challenges. *Int J Disaster Risk Reduction*, 70(15), 102771.

Reese, S., Bradley, B. A., Bind, J., Smart, G., Power, W., and Sturman, J.: Empirical building fragilities from observed damage in the 2009 South Pacific tsunami, *Earth-Sci. Rev.*, 107(1-2), 156-173, 2011.

1035   Rosti, A., Del Gaudio, C., Rota, M., Ricci, P., Di Ludovico, M., Penna, A., and Verderame, G. M. Empirical fragility curves for Italian residential RC buildings. *B. Earthq. Eng.*, 19(8), 3165-3183, 2021.

Wing, O. E., Pinter, N., Bates, P. D., and Kousky, C.: New insights into US flood vulnerability revealed from flood insurance big data, *Nat. Commun.*, 11(1), 1-10, 2020.

Pagina 12: [1] ha formattato   Hossein   09/11/2022 14:33:00

Tipo di carattere: Non Corsivo

Pagina 12: [2] ha formattato   Jalayer, Fatemeh   23/11/2022 11:52:00

Tipo di carattere: Grassetto

Pagina 12: [3] Formattato   Hossein   09/11/2022 14:50:00

Allineato al centro

Pagina 12: [4] Formattato   Hossein   13/11/2022 10:03:00

Allineato al centro, Rientro: Sinistro: 0.2 cm, Prima riga: 0 cm, Destro 0.2 cm

Pagina 12: [5] Tabella formattata   Hossein   11/11/2022 17:49:00

Tabella formattata

Pagina 12: [6] ha formattato   Hossein   11/11/2022 12:17:00

Tipo di carattere: 10 pt

Pagina 12: [7] ha formattato   Hossein   11/11/2022 12:17:00

Tipo di carattere: 10 pt

Pagina 12: [8] ha formattato   Hossein   11/11/2022 12:17:00

Tipo di carattere: 10 pt

Pagina 12: [9] ha formattato   Hossein   11/11/2022 12:17:00

Tipo di carattere: 10 pt

Pagina 12: [10] ha formattato   Hossein   11/11/2022 12:17:00

Tipo di carattere: 10 pt

Pagina 12: [11] ha formattato   Hossein   11/11/2022 12:17:00

Tipo di carattere: 10 pt

Pagina 12: [12] ha formattato   Hossein   11/11/2022 12:17:00

Tipo di carattere: 10 pt

Pagina 12: [13] ha formattato   Hossein   11/11/2022 12:17:00

Tipo di carattere: 10 pt

Pagina 12: [14] ha formattato   Hossein   11/11/2022 12:17:00

Tipo di carattere: 10 pt

| Pagina 12: [15] ha formattato | Hossein | 11/11/2022 12:17:00 |

Tipo di carattere: 10 pt

| Pagina 12: [16] ha formattato | Hossein | 11/11/2022 12:17:00 |

Tipo di carattere: 10 pt

| Pagina 12: [17] ha formattato | Hossein | 11/11/2022 12:17:00 |

Tipo di carattere: 10 pt

| Pagina 12: [18] ha formattato | Hossein | 11/11/2022 12:17:00 |

Tipo di carattere: 10 pt

| Pagina 12: [19] ha formattato | Hossein | 11/11/2022 12:17:00 |

Tipo di carattere: 10 pt

| Pagina 12: [20] ha formattato | Hossein | 11/11/2022 12:17:00 |

Tipo di carattere: 10 pt

| Pagina 12: [21] ha formattato | Hossein | 11/11/2022 12:17:00 |

Tipo di carattere: 10 pt

| Pagina 12: [22] ha formattato | Hossein | 11/11/2022 12:17:00 |

Tipo di carattere: 10 pt

| Pagina 12: [23] ha formattato | Hossein | 11/11/2022 12:17:00 |

Tipo di carattere: 10 pt

| Pagina 12: [24] ha formattato | Hossein | 11/11/2022 12:17:00 |

Tipo di carattere: 10 pt

| Pagina 12: [25] ha formattato | Hossein | 11/11/2022 12:17:00 |

Tipo di carattere: 10 pt

| Pagina 12: [26] ha formattato | Hossein | 11/11/2022 12:17:00 |

Tipo di carattere: 10 pt

| Pagina 12: [27] ha formattato | Hossein | 11/11/2022 12:17:00 |

Tipo di carattere: 10 pt

Pagina 12: [28] ha formattato	Hossein	11/11/2022 12:17:00

Tipo di carattere: 10 pt

Pagina 12: [29] ha formattato	Hossein	11/11/2022 12:17:00

Tipo di carattere: 10 pt

Pagina 12: [30] ha formattato	Hossein	11/11/2022 12:17:00

Tipo di carattere: 10 pt

Pagina 12: [31] ha formattato	Hossein	11/11/2022 12:17:00

Tipo di carattere: 10 pt

Pagina 12: [32] ha formattato	Hossein	11/11/2022 12:17:00

Tipo di carattere: 10 pt

Pagina 12: [33] ha formattato	Hossein	11/11/2022 12:17:00

Tipo di carattere: 10 pt

Pagina 12: [34] ha formattato	Hossein	11/11/2022 12:17:00

Tipo di carattere: 10 pt

Pagina 12: [35] ha formattato	Hossein	11/11/2022 12:17:00

Tipo di carattere: 10 pt

Pagina 12: [36] ha formattato	Hossein	11/11/2022 12:17:00

Tipo di carattere: 10 pt

Pagina 12: [37] ha formattato	Hossein	11/11/2022 12:17:00

Tipo di carattere: 10 pt

Pagina 12: [38] ha formattato	Hossein	11/11/2022 12:17:00

Tipo di carattere: 10 pt

Pagina 12: [39] Formattato	Hossein	11/11/2022 12:13:00

Allineato a sinistra

Pagina 12: [40] Formattato	Hossein	11/11/2022 12:13:00

Allineato a sinistra

Pagina 12: [41] Formattato	Hossein	11/11/2022 12:13:00

Allineato a sinistra

Pagina 12: [42] Formattato	Hossein	11/11/2022 17:42:00

Allineato al centro, Rientro: Prima riga: 0 cm

Pagina 12: [43] Formattato	Hossein	11/11/2022 17:29:00

Allineato a sinistra

Pagina 12: [44] Tabella formattata	Hossein	09/11/2022 14:46:00

Tabella formattata

Pagina 24: [45] ha formattato	Hossein	11/11/2022 13:18:00

Colore carattere: Blu

Pagina 24: [45] ha formattato	Hossein	11/11/2022 13:18:00

Colore carattere: Blu

Pagina 24: [45] ha formattato	Hossein	11/11/2022 13:18:00

Colore carattere: Blu

Pagina 24: [46] ha formattato	Hossein	11/11/2022 13:18:00

Colore carattere: Blu

Pagina 24: [46] ha formattato	Hossein	11/11/2022 13:18:00

Colore carattere: Blu

Pagina 24: [46] ha formattato	Hossein	11/11/2022 13:18:00

Colore carattere: Blu

Pagina 24: [47] ha formattato	Hossein	13/11/2022 09:44:00

Colore carattere: Blu

Pagina 24: [47] ha formattato	Hossein	13/11/2022 09:44:00

Colore carattere: Blu

Pagina 24: [47] ha formattato	Hossein	13/11/2022 09:44:00

Colore carattere: Blu

Pagina 24: [48] ha formattato	Hossein	13/11/2022 09:41:00

Colore carattere: Automatico

Pagina 24: [48] ha formattato   Hossein   13/11/2022 09:41:00

Colore carattere: Automatico

Pagina 24: [48] ha formattato   Hossein   13/11/2022 09:41:00

Colore carattere: Automatico

Pagina 24: [49] ha formattato   Hossein   14/11/2022 11:10:00

Colore carattere: Blu

Pagina 24: [49] ha formattato   Hossein   14/11/2022 11:10:00

Colore carattere: Blu

Pagina 24: [50] ha formattato   Hossein   14/11/2022 13:46:00

Colore carattere: Blu

Pagina 24: [50] ha formattato   Hossein   14/11/2022 13:46:00

Colore carattere: Blu

Pagina 24: [50] ha formattato   Hossein   14/11/2022 13:46:00

Colore carattere: Blu

Pagina 24: [51] ha formattato   Hossein   13/11/2022 09:41:00

Colore carattere: Automatico

Pagina 24: [51] ha formattato   Hossein   13/11/2022 09:41:00

Colore carattere: Automatico

Pagina 24: [51] ha formattato   Hossein   13/11/2022 09:41:00

Colore carattere: Automatico